Reviewed Preprint

Revised by authors after peer review.

About eLife's process

Reviewed preprint version 2
June 28, 2023 (this version)

Reviewed preprint version 1
March 24, 2023

Posted to bioRxiv
December 21, 2022

Sent for peer review
December 20, 2022

Developmental Biology

Identification of quiescent FOXC2$^+$ spermatogonial stem cells in adult mammals

Zhipeng Wang, Cheng Jin, Pengyu Li, Yiran Li, Jielin Tang, Zhixin Yu, Tao Jiao, Jinhuan Ou, Han Wang, Dingfeng Zou, Mengzhen Li, Xinyu Mang, Jun Liu, Yan Lu, Kai Li, Ning Zhang, Jia Yu, Shiying Miao, Linfang Wang, Wei Song

Department of Biochemistry and Molecular Biology, State Key Laboratory of Medical Molecular Biology, Institute of Basic Medical Sciences Chinese Academy of Medical Sciences, School of Basic Medicine Peking Union Medical College; Beijing, 100005, China • MRC Protein Phosphorylation and Ubiquitylation Unit, School of Life Sciences, University of Dundee; Dundee, DD1 5EH, UK

Abstract

In adult mammals, spermatogenesis embodies the complex developmental process from spermatogonial stem cells (SSCs) to spermatozoa. At the top of this developmental hierarchy lie a series of SSC subpopulations. Their individual identities as well as the relationships with each other, however, remain largely elusive. Using single-cell analysis and lineage tracing, we discovered both in mice and humans the quiescent adult SSC subpopulation marked specifically by forkhead box protein C2 (FOXC2). All spermatogenic progenies can be derived from FOXC2$^+$ SSCs and the ablation of FOXC2$^+$ SSCs led to the depletion of the undifferentiated spermatogonia pool. During germline regeneration, FOXC2$^+$ SSCs were activated and able to completely restore the process. Germ cell specific *Foxc2* knockout resulted in an accelerated exhaustion of SSCs and eventually led to male infertility. Furthermore, FOXC2 prompts the expressions of negative regulators of cell cycle thereby ensures the SSCs reside in quiescence. Thus, this work proposes that the quiescent FOXC2$^+$ SSCs are essential for maintaining the homeostasis and regeneration of spermatogenesis in adult mammals.

eLife assessment

This **important** study reports that Foxc2+ cells in the testis represent the quiescent spermatogonial stem cells (SSCs). The data supporting this claim are **solid**. The finding is of great significance to reproductive and stem-cell biology as male fertility depends on the fine balance between self-renewal and differentiation activities of the male germline stem cells, i.e., SSCs.

Introduction

Through spermatogenesis, spermatozoa are generated from spermatogenic cells that are originated from spermatogonial stem cells (SSCs). It is critical for this process to be continuous and successful that SSCs are maintained in a homeostatic balance between self-renewal and differentiation (S. Sharma et al., 2019). The SSCs, which belong to a subgroup of undifferentiated spermatogonia (uSPG), exhibit significant heterogeneity and dynamic characteristics. In recent years, great insights into SSC behaviors and regulations have been provided by a body of pioneer works, especially with recent advances in single-cell gene-expression profiling, highlighting great heterogeneity of SSC and focusing on characterizing the nature of SSC states. Within the population of uSPG, a number of genes relatively higher expressed in primitive subfractions have been identified and well investigated, i.e., *Gfra1*, *ID4*, *Ret*, *Eomes*, *Pax7*, *Nanos2*, *Shisa6*, *T*, *Pdx1*, *Lhx1*, *Egr2* and *Plvap* (Aloisio et al., 2014; Guo et al., 2004; Hara et al., 2014; Helsel et al., 2017; Jijiwa et al., 2008; La et al., 2018; Nakagawa et al., 2021; Oatley et al., 2007; Sada et al., 2009; M. Sharma et al., 2019; Tokue et al., 2017). Particularly, *Gfra1*, *ID4*, *Eomes*, *Pax7*, *Nanos2*, and *Plvap* are further validated through lineage tracing experiment, which is considered to be a reliable method to study the development of stem cells. However, some essential and primitive sub-populations remain undiscovered, and the identification of which is of great significance for elucidating the developmental process of SSC renewal and its behavior in testis.

Adult stem cells (ASCs), as the undifferentiated primitive cells that can be found in nearly all types of tissues in mammals, are characteristic for a unique quiescent status reflected by both reversible cell cycle arrest and specific metabolic alterations (van Velthoven & Rando, 2019). The role of the quiescent stem cells is to avoid premature exhaustion and to allow the long-term maintenance of a functional stem cell pool (Cheung & Rando, 2013). The adult SSCs appear to share this characteristic, as revealed in recent single-cell RNA-sequencing (scRNA-seq) analysis in humans and mice, being largely non-proliferative while capable of reciprocating between the quiescent and activated status during homeostasis and regeneration (Guo et al., 2018; Hermann et al., 2018; Suzuki et al., 2021; Tan & Wilkinson, 2019; Wang et al., 2018). This notion has also been significantly supported by the discoveries of important regulators such as USF1 (Faisal et al., 2019) and DNMT3L (Liao et al., 2014) as well as the pathways including the PI3K/MAPK and mTORC1 signalings (Suzuki et al., 2021). In addition, it is generally believed that cells in a quiescent state are supposed to be more resilient to genotoxic insults, thus theoretically the quiescent SSCs can restore spermatogenesis upon such disturbance. However, by large, much remain unknown as to the characteristics and regulation of the quiescence state of adult SSCs. Thus, more important insights can be obtained through searching the quiescent SSC population and defining the essential characteristics of this population as the foundation of successful spermatogenesis.

Forkhead box protein C2 (FOXC2), a member of the forkhead/winged helix transcription factor family, plays essential roles in the development of various tissues in mice (Bahuau et al., 2002; Kume et al., 2001; Motojima et al., 2016; Sasman et al., 2012). Recently, FOXC2 has been found to be expressed in A_s and A_{pr} spermatogonia of mouse testes and is required for SSC maintenance (Wei et al., 2018). However, the role of FOXC2 in the development of adult SSCs *in vivo* has yet to be explored. In this study, we identified a subpopulation of adult SSCs specifically expressed by FOXC2. In adult mice, FOXC2$^+$ SSCs gave rise to all spermatogenic progenitor cells that can complete the full spermatogenesis. Upon the loss of FOXC2$^+$ SSCs, the undifferentiated spermatogonia pool was exhausted, eventually leading to defective spermatogenesis. Specifically, FOXC2 is required for maintaining SSC quiescence by promoting the expression of negative regulators of cell cycle. Moreover, the FOXC2$^+$ population endured the chemical insult with busulfan and effectively restored

spermatogenesis. Overall, we propose that FOXC2^{+} represents the quiescent state of the SSCs in adult mammals that is crucial for the homeostasis and regeneration of SSCs.

Results

Identification of FOXC2^{+} SSCs from the adult uSPGs

We performed single-cell RNA-seq (10x genomics) of the uSPG from adult mice testes marked by THY1, a widely recognized surface marker for uSPG with self-renewing and transplantable state (Hammoud et al., 2014; Kubota et al., 2004), to dissect the heterogeneity and developmental trajectory (Figure 1A, Figure 1—figure supplement 1A, B). Among 5 distinct clusters identified, Cluster1 was characterized by the high expression of stemness markers whereas other clusters were featured by progenitor or differentiating spermatogonia (dSPG) markers (Figure1B, Figure 1—figure supplement 1C, D). Primarily mapped to the extreme early point of the developmental trajectory, Cluster1 cells appeared quiescent and likely represented the primitive state of uSPG populations (Figure1B, Figure 1—figure supplement 1E-G). The top10 differentially expressed genes (DEGs) associated with Cluster1 are featured by SSC markers such as *Mcam* (Kanatsu-Shinohara et al., 2012), *Gfra1* (Hara et al., 2014), *Tcl1* and *Egr2* (Hermann et al., 2018; La et al., 2018) (Figure1C, Figure 1—figure supplement 2A, Figure 1—source data 1) in addition to six others expressed in different stages of germ cells and/or somatic cells, in which only FOXC2 was exclusively localized in the nucleus of a subgroup of ZBTB16^{+} uSPG in mice (Buaas et al., 2004; Costoya et al., 2004) (Figure 1D, Figure 1—figure supplement 2B). More specifically, FOXC2 displayed differential expressions among various subtypes of uSPG, being more specific in A_s (59.9%) than other subtypes including A_{pr} (5.2%), A_{pr-1} (4.1%), A_{al4-1} (1.83%), A_{al8-1} (1.5%), and A_{al16-1} (1.67%) (Figure 1E). There was only a small fraction (5.1%) was active in proliferation as indicated by MKI67 (Figure 1F), suggesting that FOXC2^{+} cells are primarily quiescent. Additionally, when examining the SSC markers validated previously by lineage tracing (La & Hobbs, 2019), we found that FOXC2 displays a higher level of co-localization with GFRA1 and EOMES than PAX7 and NEUROG3 (Nakagawa et al., 2007), indicating the FOXC2^{+} cells contain but differ from the known SSC subsets (Figure 1G).

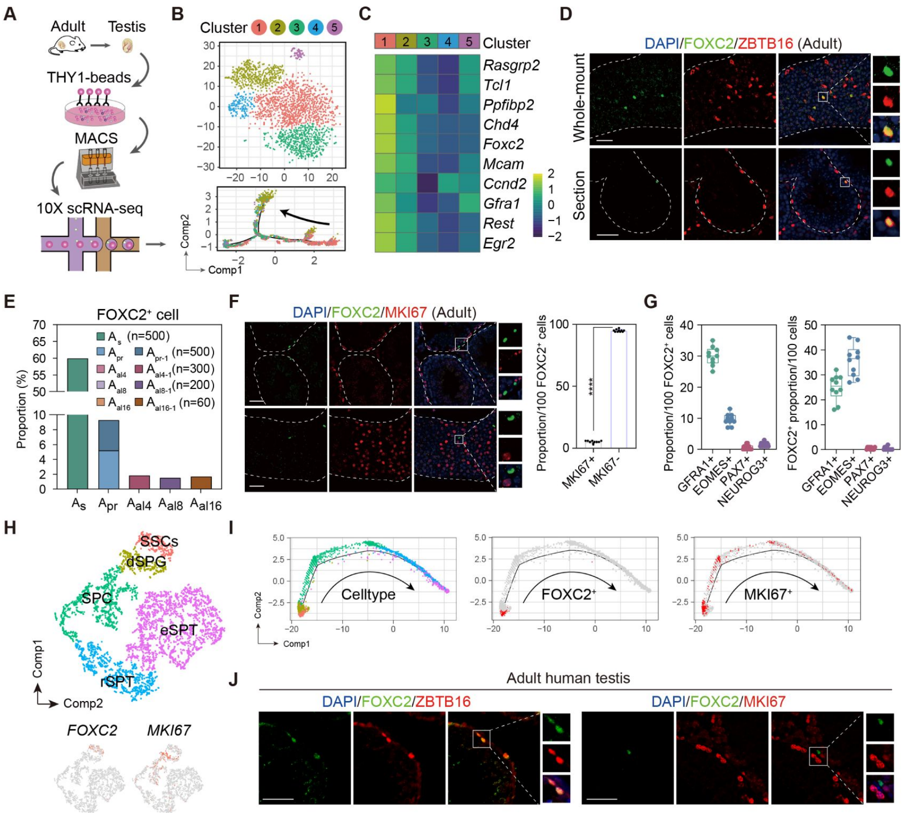

Figure 1

Identification of the FOXC2^{+} SSCs in adult mouse and human testis.

(**A**) Schematic illustration of the single-cell analysis workflow. (**B**) t-SNE plot and developmental trajectory of all uSPG, colored by cluster. (**C**) Heatmap of the Top10 DEGs in Cluster1. (**D**) Immunostaining for ZBTB16 (red), FOXC2 (green), and DAPI (blue) in testicular paraffin sections from wild-type adult C57 mice. Scale bar, 50 μm; C57, C57BL/6J. (**E**) The proportion of FOXC2^{+} cells in different uSPG subtypes. (**F**) Immunostainings for MKI67 (red), FOXC2 (green), and DAPI (blue) in adult mice testis and the proportion of MKI67^{+} cells in FOXC2^{+} population (n=10). Scale bar, 50 μm; values, mean ± s.e.m.; p-values were obtained using two-tailed t-tests (****p-value < 0.0001). (**G**) The co-expression proportion between the FOXC2 and differential known SSCs makers (n=10). (**H**) t-SNE plot of germ cells in adult human testis (GSE112013), colored by germ cell type. Feature plot showing the expression patterns of FOXC2 and MKI67 in human germ cells. (**I**) The developmental trajectory of the human germ cells, colored by germ cell type, FOXC2 expression cells (red), or MKI67 expression cells (red). (**J**) Immunostaining for ZBTB16/MKI67 (red), FOXC2 (green), and DAPI (blue) in testicular paraffin sections from adult humans.

We next analyzed the expression of FOXC2 in adult human testis using the published scRNA-seq dataset (GSE112013) (Guo et al., 2018). As expected, FOXC2 was also specifically expressed in the human SSCs, most of which were MKI67^{-} (Figure 1H, Figure 1—figure supplement 2C). Pseudotime analysis showed that the FOXC2^{+} cells located at the start of the developmental trajectory with a proportion of about 90% that were MKI67^{-} (Figure 1I). Immunofluorescence staining confirmed that FOXC2^{+} cells were a subset of ZBTB16^{+} spermatogonia in adult human testis, and most of them were MKI67^{-} (Figure 1J), representing a quiescent subpopulation of SSCs in human testis(Clermont, 1966a, 1966b, 1969; Ehmcke & Schlatt, 2006; Ehmcke et al., 2006). These results suggest that FOXC2 is similarly expressed in the SSCs of adult human and mouse testis and may possess a conserved function.

FOXC2^{+} SSCs sufficiently initiate and sustain spermatogenesis

We generated *Foxc2*$^{iCreERT2/+}$;*Rosa26*$^{LSL\text{-}T/G/LSL\text{-}T/G}$ mice in which FOXC2^{+} cells were specifically labeled with GFP to enable the progeny tracing after tamoxifen treatment (Figure 2—figure supplement 1) (Wang et al., 2015). Tamoxifen was introduced at 2-month of age,

after which the FOXC2-expressing lineage (GFP^{+}) was tracked at d3 (day3), w1 (week1), w2, w4, w6, m4 (month4), m7, and m12 respectively (Figure 2A). At d3, the tracked cells were both GFP^{+} and FOXC2^{+} (Figure 2B) and constituted 0.027% of the total testicular cells as indicated by the fluorescence-activated cell sorting (FACS) analysis (Figure 2C). GFP^{+} cells and THY1^{+} cells sorted by FACS were then transplanted into testes of recipient mice pre-treated with busulfan, respectively. Two months after transplantation, FOXC2^{+} cells generated 3.6 times greater number of colonies than the THY1^{+} control (Figure 2D, E), indicating that the FOXC2^{+} cells possess higher stemness as convinced by stronger transplantable viability.

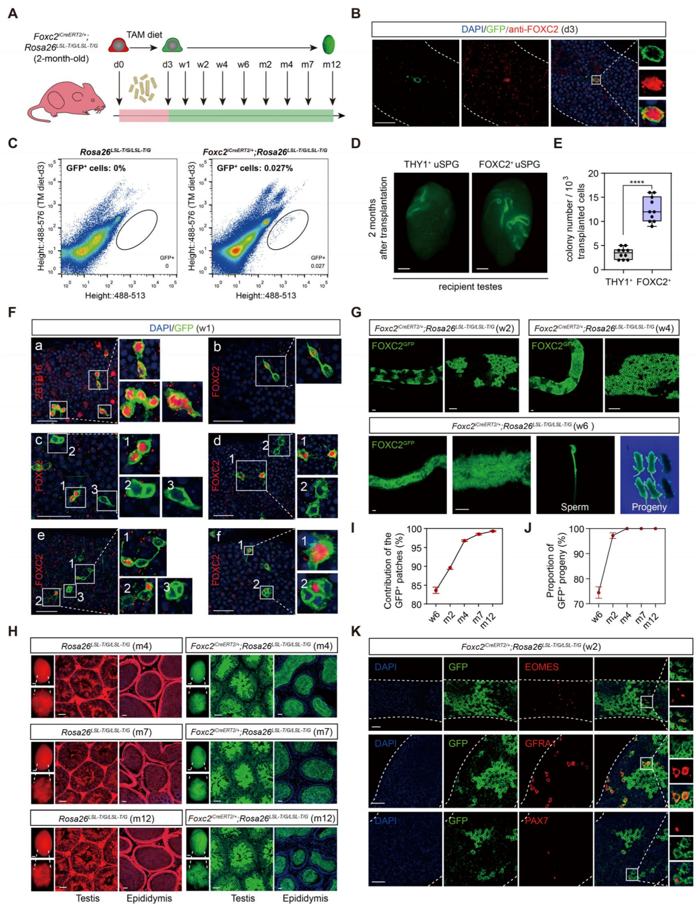

Figure 2

Lineage tracing and functional validation of FOXC2^{+} SSCs in *Foxc2$^{iCreERT2/+}$;Rosa26$^{LSL-T/G/LSL-T/G}$* mice.

(**A**) Schematic illustration of the lineage tracing workflow for FOXC2^{+} cells. (**B**) Immunostainings for DAPI (blue) and FOXC2 (red) at day 3 post TAM induction. Scale bar, 50 μm; d, day. (**C**) FACS analysis of GFP^{+} populations derived from *Rosa26$^{LSL-T/G/LSL-T/G}$* or testes (**D**) and colony numbers (**E**) 2 months after transplantation (n=10) of the FACS-sorted GFP^{+} cells from the *Foxc2$^{iCreERT2/+}$;Rosa26$^{LSL-T/G/LSL-T/G}$* mice 3 days after TAM diet and the FACS-sorted THY1^{+} cells from adult mice. Scale bar, 1 mm; values, mean ± s.e.m.; p-values were obtained using two-tailed t-tests (****p-value < 0.0001). (**F**) Immunostaining for DAPI (blue), ZBTB16/FOXC2 (red), and GFP (green) at week 1 post TAM induction (scale bar, 50 μm). (**G**) Seminiferous tubules of *Foxc2$^{iCreERT2/+}$;Rosa26$^{LSL-T/G/LSL-T/G}$* mice 2, 4, and 6 weeks post TAM induction. Scale bar, 50 μm. **(H)** Testes (scale bar, 1 mm), seminiferous tubules, and epididymis (scale bar, 50 μm) at month 4, 7, and 12 post TAM induction in *Foxc2$^{iCreERT2/+}$;Rosa26$^{LSL-T/G/LSL-T/G}$* mice. (**I**, **J**) The GFP^{+} patches **(I)** and progeny (**J**) population dynamics (n=10). Values, mean ± s.e.m. (**K**) Immunostainings for DAPI (blue), EOMES (red), GFRA1 (red), or PAX7 (red) in GFP^{+} population at week 2 post TAM induction. Scale bar, 50 μm.

At w1, all GFP^{+} cells were identified as uSPGs, encompassing A_s, A_{pr}, and $A_{al\text{-}4}$ (Figure 2F$_a$). Specifically, FOXC2^{+} A_s gave rise to 3 types of A_{pr}, i.e., FOXC2^{+}/FOXC2^{+}, FOXC2^{+}/FOXC2^{-}, and FOXC2^{-}/FOXC2^{-} (Figure 2F$_{c1,\ b,\ c2,\ d2}$), which then either produced FOXC2^{+} or FOXC2^{-} A_s through symmetric or asymmetric division (Figure 2F$_{c3,\ d1,\ f1}$), or developed into A_{al} with no more than one FOXC2^{+} cell in the chains (Figure 2F$_{e,\ f2}$). These results confirm that FOXC2^{+} cells are capable of self-renewal to sustain the population as well as replenishing the uSPG pool by producing downstream progenies, thereby serving as SSCs. In the following 2-6 weeks, GFP^{+} colonies further expanded and produced GFP^{+} sperms in the epididymis, from

of the seminiferous tubules at w6, m2, m4, m7, and m12 respectively (Figure 2H, I). All offspring were GFP^{+} from m4 onwards (Figure 2J). Additionally, the EOMES^{+}, GFRA1^{+} and PAX7^{+} cells were all GFP^{+} at w2, further confirming these progenies were derived from the FOXC2^{+} cells (Figure 2K). Overall, FOXC2^{+} SSCs can produce all subtypes of uSPG, thus initiating spermatogenesis in adult mice.

Specific ablation of the FOXC2^{+} SSCs results in the depletion of uSPG pool

We then prepared *Foxc2*$^{iCreERT2/+}$;*Rosa26*$^{LSL\text{-}DTA/+}$ mice to investigate the physiological requirement of FOXC2^{+} SSCs in spermatogenesis (Wang et al., 2015). FOXC2^{+} population in 2-month-old mice was specifically ablated with tamoxifen-induced diphtheria toxin (DTA). The testes of these mice were examined at d3, d7, and d14 post tamoxifen induction (Figure 3A). Gradual loss of weight in testes coincided with the reduction in the size of testes in all the mice while body weight was maintained (Figure 3B, C). Specifically, at d3, there were no detectable FOXC2^{+} cells in addition to the decrease in the number of GFRA1^{+}, LIN28A^{+} (Zheng et al., 2009) and ZBTB16^{+} uSPG at the basement membrane of seminiferous tubules; at d14, all GFRA1^{+}, LIN28A^{+} and ZBTB16^{+} uSPG disappeared while vacuoles formed at the basement membrane with remaining spermatocytes and spermatids in the seminiferous lumen (Figure 3D–F, Figure 3—figure supplement 1). Meanwhile, the expression of DDX4 (Toyooka et al., 2000) and DAZL (Li et al., 2019) as germ cell markers was significantly reduced along with nearly undetectable expression of uSPG markers such as ZBTB16, LIN28A, GFRA1, RET, and NEUROG3 (Nakagawa et al., 2007) (Figure 3G). These results indicate an uSPG exhaustion as the result of the FOXC2^{+} SSCs ablation, therefore supporting the critical role played by FOXC2^{+} population in spermatogenesis.

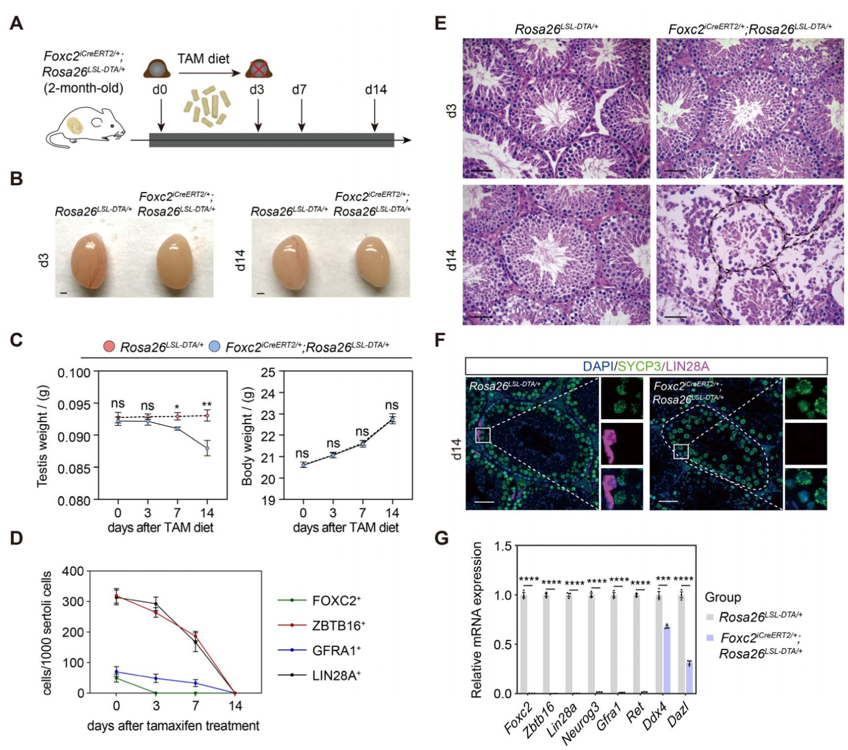

Figure 3

Specific ablation of FOXC2^{+} SSCs and phenotypic validation in *Foxc2*$^{iCreERT2/+}$;*Rosa26*$^{LSL\text{-}DTA/+}$mice.

(**A**) Schematic illustration of the lineage tracing workflow for FOXC2^{+} cells. (**B-D**) Phenotypic validation of the *Rosa26*$^{LSL\text{-}DTA/+}$ and *Foxc2*$^{iCreERT2/+}$;*Rosa26*$^{LSL\text{-}DTA/+}$ mice (n=5) for testes size (**B**), testis weight and body weight (**C**), and HE-staining of the testes (**D**). Scale bars in (**B**), 1 mm; in (**D**), 50 μm; d, day; values were mean ± s.e.m.; p-values were obtained using two-tailed t-tests (ns > 0.05, *p-value < 0.05, **p-value < 0.01). (**E**) ZBTB16^{+}, GFRA1^{+}, LIN28A^{+}, and FOXC2^{+} SPG populations dynamics. Values, mean ± s.e.m. (n=10); p-values were obtained using one-way ANOVA followed by Tukey test (ns > 0.05, *p-value < 0.05, **p-value < 0.01, ****p-value < 0.0001). (**F**) Immunostainings for DAPI (blue), SYCP3 (green), and LIN28A (magenta) at day 14 post TAM induction. d, day; scale bar, 50 μm. (**G**) Quantitative RT-PCR analysis of SPG markers expression in the testes of the *Rosa26*$^{LSL\text{-}DTA/+}$ and *Foxc2*$^{iCreERT2/+}$;*Rosa26*$^{LSL\text{-}}$

DTA/+ mice (n=3). Values, mean ± s.e.m.; p-values were obtained using two-tailed t-tests (***p-value < 0.001, ****p-value < 0.0001).

FOXC2$^+$ SSCs are resistant to busulfan and indispensable for germline regeneration

Next, we examined the regenerative viability of FOXC2$^+$ SSCs. At d20 post busulfan treatment (20mg/kg), FOXC2$^+$ cells constituted the majority of uSPGs (Figure 4A). Following a sharp decrease in cell number in the first five days, ZBTB16$^+$ and GFRA1$^+$ cells began to recover from d25 while the number of FOXC2$^+$ cells remained stable (Figure 4B), indicating that this population is insensitive to busulfan. We then checked changes in the proportion of MKI67$^+$ cells in FOXC2$^+$ population after busulfan treatment (Figure 4C, D). At d30, the MKI67$^+$ proportion rose to 15.92%, indicating a higher level of proliferation, albeit the total cell number stayed static (Figure 4B, D), thereby becoming the driving force in restoring spermatogenesis. Up to d120, the MKI67$^+$ proportion had settled gradually back to the pre-treatment level, accompanied by the full recovery of spermatogenesis (Figure 4D). Further details of this process were revealed during lineage tracing (Figure 4E). Three days after tamoxifen induction, the 2-month-old *Foxc2$^{iCreERT2/+}$;Rosa26$^{LSL-T/G/LSL-T/G}$* mice were treated with busulfan. Consistent with the results above, at d20, the survived uSPGs were predominantly GFP$^+$ (Figure 4F). Over 68.5% of the total length of the seminiferous tubules were GFP$^+$ at m2, and this proportion rose to 95.43%, 98.41%, and 99.27% at m4, m7, and m12 respectively (Figure 4G, H), which was comparable to the proportion by tamoxifen induction alone (Figure 2I). From m4 onwards, nearly all germ cells, spermatids, and their offspring were GFP$^+$ (Figure 4G, I). Together, these results confirm that FOXC2$^+$ SSCs are indispensable for germline regeneration that is central to spermatogenesis recovery from interruptions.

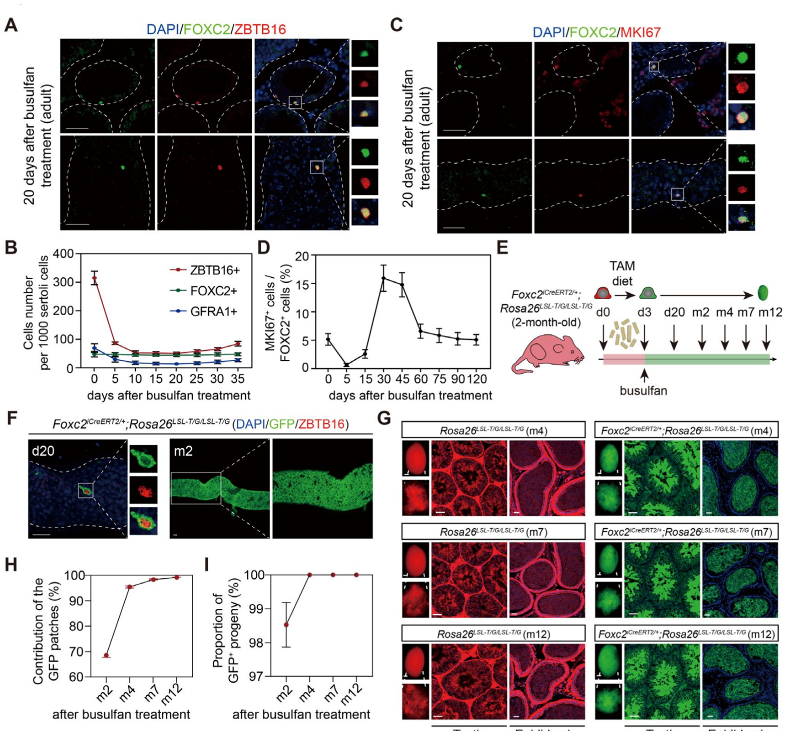

Figure 4

FOXC2$^+$ SSCs are critical for germline regeneration.

(**A**) Co-immunostaining of FOXC2 (green) with ZBTB16 (red) in seminiferous tubules of the adult testes at day 20 post busulfan treatment. Scale bar, 50 μm. (**B**) ZBTB16$^+$, GFRA1$^+$, and FOXC2$^+$ population dynamics after busulfan treatment (20 mg/kg, n=10). (**C**) Co-immunostaining of FOXC2 (green) with MKI67 (red) in seminiferous tubules of the adult testes at day 20 post busulfan treatment. Scale bar, 50 μm. (**D**) MKI67$^+$FOXC2$^+$ proportions in relation to the whole FOXC2$^+$ population at different time points after busulfan treatment (n=4). (**E**) Schematic illustration for lineage tracing of FOXC2$^+$ cell after busulfan treatment. (**F**) Lineage tracing of the GFP$^+$ cells at day 20 and month 2 after busulfan treatment (scale bar, 50 μm). (**G**) The testes (scale bar, 1 mm),

seminiferous tubules, and epididymis (scale bar, 50 μm) at month 4, 7, and 12 post TAM induction and busulfan injection. m, month. (**H**, **I**) The proportion dynamics of GFP patches (**H**) and GFP^{+} progenies (**I**). Values, mean ± s.e.m. (n=10). w, week; m, month.

FOXC2 is essential for SSC maintenance in adult mice

We then focused on dissecting the role of FOXC2 in the SSC maintenance using *Foxc2$^{f/-}$;Ddx4$^{Cre/+}$* mice (Gallardo et al., 2007) (Figure 5A). No significant difference was observed in the expressions of various uSPG markers, including ZBTB16 and LIN28A, between *Foxc2$^{f/-}$;Ddx4$^{Cre/+}$* and *Foxc2$^{f/+}$* mice at the age of 1 week (Figure 5—figure supplement 1A). However, adult *Foxc2$^{f/-}$;Ddx4$^{Cre/+}$* mice displayed clear testis weight loss without significant body weight loss (Figure 5B, C). Moreover, in these mice, we observed severe degeneration of seminiferous tubules, reduced number of spermatids in the epididymis, and decreased size of the uSPG population with age (Figure 5D–G) but without apparent signs of apoptosis (Figure 5—figure supplement 1B). The 6-month-old *Foxc2$^{f/-}$;Ddx4$^{Cre/+}$* mice were infertile, in which over 95% seminiferous tubules were Sertoli-only with hardly detectable expressions of DAZL, DDX4, LIN28A, and ZBTB16 (Figure 5D–F, H). Therefore, FOXC2 is essential for maintaining the SSC homeostasis and normal spermatogenesis in adult mice.

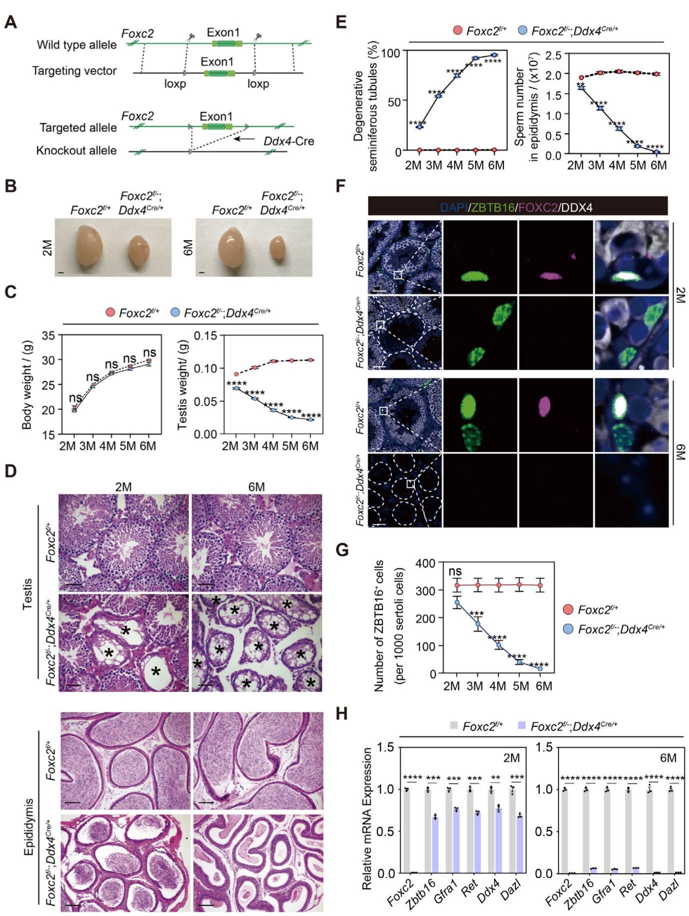

Figure 5

Spermatogenesis exhaustion in the adult *Foxc2$^{f/-}$;Ddx4$^{Cre/+}$* mice.

(**A**) Construction of the *Foxc2$^{f/-}$;Ddx4$^{Cre/+}$*mice. (**B**) The testes size of the *Foxc2$^{f/-}$;Ddx4$^{Cre/+}$*mice. Scale bar, 1mm; M, month. (**C**) Body weight and testis weight of the *Foxc2$^{f/-}$;Ddx4$^{Cre/+}$*mice at different age (n=5). M, month; values, mean ± s.e.m.; p-values were obtained using two-tailed t-tests (ns > 0.05, ****p-value < 0.0001). (**D**) HE-staining of the testis and epididymis. Scale bar, 50 μm; M, month. (**E**) *Foxc2$^{f/-}$;Ddx4$^{Cre/+}$*mice with age (n=5). Values, mean ± s.e.m.; p-values were obtained using two-tailed t-tests (**p-value < 0.01, ****p-value < 0.0001). (**F**) Immunostainings for DAPI (blue), ZBTB16 (green), FOXC2 (magenta), and DDX4 (white) in the seminiferous tubules of the *Foxc2$^{f/+}$* and *Foxc2$^{f/-}$;Ddx4$^{Cre/+}$*mice. Scale bar, 50 μm. (**G**) Estimation of ZBTB16^{+} uSPG number in the *Foxc2$^{f/+}$* and *Foxc2$^{f/-}$;Ddx4$^{Cre/+}$*mice with age (n=5). Values, mean ± s.e.m.; p-values were obtained using two-tailed t-tests (ns > 0.05, ***p-value < 0.001, ****p-value < 0.0001). (**H**) Quantitative RT-PCR analysis of the uSPG and germ cell markers expressed in the testis of the *Foxc2$^{f/+}$* and *Foxc2$^{f/-}$;Ddx4$^{Cre/+}$*mice (n=3). M, month; values, mean ± s.e.m.; p-values were obtained using two-tailed t-tests (**p-value < 0.01, ***p-value < 0.001, ****p-value < 0.0001).

FOXC2 maintains the quiescent state of SSCs through negatively regulating the cell cycle

We collected THY1^{+} uSPGs from 4-month-old *Foxc2*$^{f/+}$and *Foxc2*$^{f/-}$;*Ddx4*$^{Cre/+}$ mice and compared their transcriptome signatures revealed from scRNA-seq (Figure 6A). The pseudotime analysis identified Cluster1, which represented the FOXC2-expressing SSCs in *Foxc2*$^{f/+}$mice corresponding to the FOXC2-deleting SSCs in the *Foxc2*$^{f/-}$;*Ddx4*$^{Cre/+}$mice, was specifically assigned to the extremely early stage of the development trajectory in respective samples, which was validated by the expression of corresponding markers (Figure 6B, Figure 6—figure supplement 1A, B). Aggregated analysis of the overall uSPG populations showed that cells derived from *Foxc2*$^{f/-}$;*Ddx4*$^{Cre/+}$mice were specifically associated with the late stage of the development trajectory, as opposed to *Foxc2*$^{f/+}$mice where nearly all the cells derived were concentrated at the early stage of development (Figure 6C, Figure 6—figure supplement 1C). This implies that the loss of FOXC2 prompts the SSCs to progress into a more differentiated stage. Further analysis of the cells in Cluster1 revealed two distinct subclusters, i.e., Subclusters0 and Subclusters1 (Figure 6— figure supplement 2A). Formed primarily by the Cluster1 cells derived from *Foxc2*$^{f/+}$mice, Subclusters0 was featured by stemness markers, while Subcluster1, representing the majority of Cluster1 cells from *Foxc2*$^{f/-}$;*Ddx4*$^{Cre/+}$mice, was featured by progenitor markers (Figure 6—figure supplement 2B, C). Consistently, pseudotime analysis showed that Cluster1 cells from *Foxc2*$^{f/+}$ mice projected a forward stage of the developmental trajectory indicated by stemness markers, whereas Cluster1 cells from *Foxc2*$^{f/-}$;*Ddx4*$^{Cre/+}$ mice were associated with a later stage of the developmental trajectory (Figure6D, Figure 6—figure supplement 2D, E). More specifically, less number of cells were found at the starting state1 in Cluster1 from *Foxc2*$^{f/-}$;*Ddx4*$^{Cre/+}$ mice than in *Foxc2*$^{f/+}$mice, with rather more cells in the developmental progression (from state1 to state5), especially at the advanced state5 (Figure 6E). Thus, FOXC2 deletion caused defective SSC maintenance and committed the SSCs to a differentiation destiny. Further, there were 932 genes down-regulated in Cluster1 cells derived from *Foxc2*$^{f/-}$;*Ddx4*$^{Cre/+}$mice in comparison to *Foxc2*$^{f/+}$ mice (Figure 6F, Figure 6—source data 1), which were functionally associated with both stem cell population maintenance and mitotic cell cycle (Figure 6G). Consistently, the GSEA analysis revealed a more progressive cell cycle in Cluster1 upon *Foxc2*-knockout (Figure 6H), confirming the role of FOXC2 in regulating the cell cycle of the SSCs.

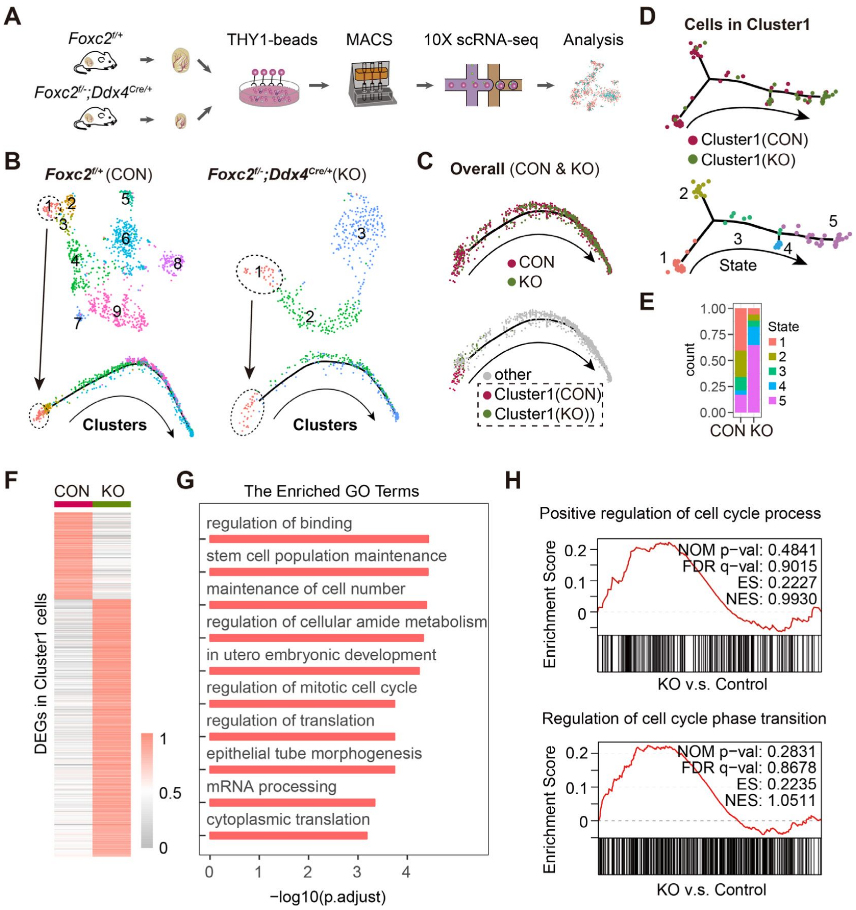

Figure 6

scRNA-seq analysis of THY1^{+} uSPG in *Foxc2$^{f/+}$* and *Foxc2$^{f/-}$;Ddx4$^{Cre/+}$* mice.

(**A**) Schematic illustration of the scRNA-seq workflow. (**B**) t-SNE plot and developmental trajectory of uSPG from *Foxc2$^{f/+}$* and *Foxc2$^{f/-}$;Ddx4$^{Cre/+}$* mice respectively, colored by cluster. (**C**) Developmental trajectories of uSPG from *Foxc2$^{f/+}$* and *Foxc2$^{f/-}$;Ddx4$^{Cre/+}$* mice, colored by sample or derivation. (**D**) Developmental trajectories of the cells in Cluster1 from *Foxc2$^{f/+}$* (CON) and *Foxc2$^{f/-}$;Ddx4$^{Cre/+}$*(KO) mice, colored by derivation or developmental state. (**E**) The Cluster1 cells proportion of each state in CON and KO mice. (**F**) Heatmap showing the DEGs in the Cluster1 cells from the *Foxc2$^{f/-}$;Ddx4$^{Cre/+}$* mice compared with the *Foxc2$^{f/+}$* mice. (**G**) Top GO terms enrichment by the down-regulated DEGs in KO mice. (**H**) Gene set enrichment analysis (GSEA) of the Cluster1 cells (*Foxc2$^{f/-}$;Ddx4$^{Cre/+}$* v.s. *Foxc2$^{f/+}$* mice).

NOM, nominal; FDR, false discovery rate; ES, enrichment score; NES, normalized enrichment score.

We then performed Cleavage Under Targets and Tagmentation (CUT&Tag) sequencing to explore the underlying mechanism (Kaya-Okur et al., 2020; Kaya-Okur et al., 2019), for which GFP^{+} SSCs from *Foxc2$^{iCreERT2/+}$;Rosa26$^{LSL-T/G/LSL-T/G}$* mice 3 days after tamoxifen induction, representing the FOXC2^{+} SSCs, were isolated for CUT&Tag sequencing (Figure 7A). Specific peaks enriched in the promoter region of 3629 genes (Figure 7B, C; Figure 7—source data 1) showed functional enrichment in biological processes such as DNA repair and mitotic cell cycle regulation (Figure 7D). By overlapping with the 932 genes down-regulated in Cluster1 cells from *Foxc2$^{f/-}$;Ddx4$^{Cre/+}$* mice, we obtained 306 genes as the candidates subjective to the regulation by FOXC2 (Figure 7E; Figure 7—source data 1). Further, Gene Ontology (GO) enrichment analysis of these genes highlighted a distinctive functional cluster (11 genes) focusing on the negative regulation of cell cycle (Figure 7F; Figure 7—source data 1) (Bahar et al., 2002; Bakker et al., 2004; Gaudet et al., 2011; Georgescu et al., 2014; Knudson & Korsmeyer, 1997; Nitiss, 2009; Raman et al., 2007; van Oosten et al., 2005; Weaver et al., 2003; Yi et al., 2012). More specifically, significant peaks enrichment at the promoter region were observed for these candidate genes (Figure 7G). Meanwhile, as predicted using the JASPAR Scan function (binding potential >0.8), there showed strong binding potential of FOXC2 towards these candidate genes (Figure 7I) via the binding motif of FOXC2 (Figure 7H), which was further confirmed by the result from the CUT&Tag qPCR (Figure 7J). Overall results imply that FOXC2 may function as a gatekeeper that ensures the quiescent state of SSCs by impeding cell cycle progression.

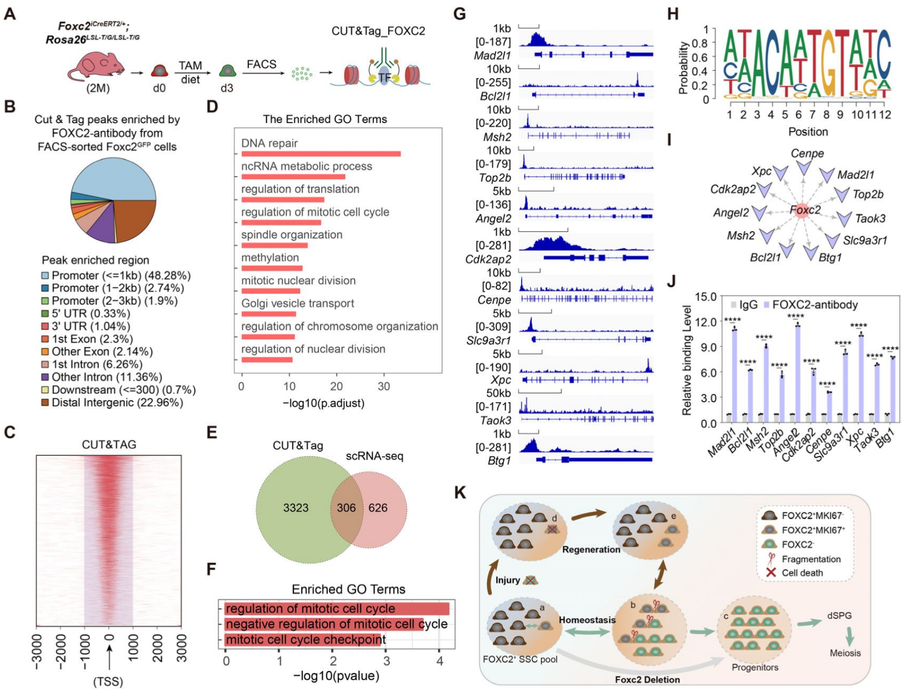

Figure 7

FOXC2 is essential for sustaining the quiescent state of SSCs via regulating cell cycle.

(**A**) Workflow schematic illustration of the CUT&Tag_FOXC2 analysis on the FACS-sorted FOXC2^{+} cells. (**B**) Pie chart for CUT&Tag_FOXC2 peaks genome distribution. (**C**) Profiling of CUT&Tag_FOXC2 peaks in proximity to transcriptional starting site (TSS). The distance to TSS within 1000 was highlighted in the purple box. (**D**) Top GO terms enrichment by genes annotated by CUT&Tag_FOXC2 peaks. (**E**) Venn diagram of FOXC2 target genes defined by overlapping the CUT&Tag sequencing and scRNA-seq datasets. (**F**) GO terms enrichment by the FOXC2 target genes related to cell cycle regulation. (**G**) Chromatin landscapes of CUT&Tag_FOXC2 peaks of the candidates associated with negative cell cycle regulation. (**H**) The DNA-binding motif for FOXC2 (predicted with HOMER). (**I**) The cell cycle-related candidates possessing high binding potential (>0.8, predicted with JASPAR SCAN). (**J**) CUT&Tag-qPCR validation of the cell cycle arrest regulatory genes. (n=3). Values, mean ± s.e.m.; p-values were obtained using two-tailed t-tests (****p-value < 0.0001). (**K**) The model for the maintenance of the FOXC2^{+} SSC subpopulation in adult testis.

Figure 7—source data 1. Excel spreadsheet with the list of the differentially expressed genes found by CUT&Tag sequencing and Gene Ontology terms of the 306 crossed candidates.

Discussion

In this work, a comprehensive analysis of uSPG populations with scRNA-seq and the following lineage tracing study by whole-mount immunofluorescence assay led to the identification of FOXC2^{+} SSCs as a quiescent SSC subpopulation in adult mice. Further investigation through functionality analysis confirmed FOXC2 is essential for SSC self-renewal and stemness, thereby is required for maintaining the SSC population that is critical for continuous spermatogenesis. Importantly, our data demonstrated that the colonies formed by FOXC2^{+} cells constituted nearly the total length of the seminiferous tubules (99.31%), implying that the FOXC2^{+} SSCs can support the complete spermatogenesis in adult mice.

GFRA1^{+} A_{pr} and A_{al} cells are found to break randomly and a portion of them can return to the stem cell state (Hara et al., 2014). Interestingly, our findings showed FOXC2 appeared in one of the A_{pr} or A_{al} cells at times, therefore raising a possibility that the subset of GFRA1^{+} cells that return to stem cell state after intercellular bridge break, maybe FOXC2^{+} due to different cell cycle state. If so, based on both findings, GFRA1^{+}FOXC2^{+} could represent a

quiescent state whereas GFRA1^{+}FOXC2^{-} is proliferate active, which certainly requires further validation possibly through multiple lineage tracing and live imaging.

We observed that the FOXC2^{+} SSCs were almost all in a non-proliferative state (~94.9%), and further revealed that FOXC2 functioned in the negative regulation of cell cycle progression, thus confirming that FOXC2-expressing SSCs are quiescent SSC population in adult mice. The finding that FOXC2 inhibited cell cycle and differentiation of SSCs in testis is consistent with that reported in other tissues (Davis et al., 2004; Sabine et al., 2015). In general, the quiescent state is a protective mechanism for stem cell storage and prevents stem cells from damage or depletion under genotoxic stresses (Arai & Suda, 2007; Relaix & Zammit, 2012; Rodgers et al., 2014; S. Sharma et al., 2019). In our work, after the busulfan treatment, the quantity of FOXC2^{+} cells remained stable and the survived uSPGs were predominantly FOXC2^{+}, indicating its insensitivity to cytotoxic agents. However, the proportion of MKI67^{+}FOXC2^{+} cells increased by 15.92% after 30 days of the busulfan treatment and decreased back to the pre-treatment level (5.08%) at 120 days, implying that the quiescent FOXC2^{+} cells are able to transform into the proliferative FOXC2^{+} cells to replenish the SSC pool to maintain the SSC homeostasis and normal spermatogenesis. We further confirmed by lineage tracing analysis that FOXC2-expressing cells were the only remaining SSC population and were responsible for germline regeneration after the busulfan treatment, indicating that FOXC2^{+} SSCs represent a functionally important stem cell population with regenerative ability. In the future, more insights into the unique regulation of SSCs can be drawn from studying and comparing the transition between the quiescent and proliferative states in FOXC2^{+} and other SSC subpopulations.

According to our findings, we propose a model for the maintenance of the FOXC2^{+} SSC subpopulation (Figure 7K). Under physiological conditions, FOXC2^{+} A_s cells (including FOXC2^{+}GFRA1^{+}, FOXC2^{+}EOMES^{+} cells, etc.) constitute the SSC pool, of which only a small proportion (~5.1%) cells are proliferative while the majority remains quiescent (Figure 7Ka). This population can divide symmetrically or asymmetrically into different A_{pr} and A_{al} (Figure 7Kb). Then FOXC2^{+} cells (Figure 7Kb) may break from the syncytial and return to A_s state (Figure 7Ka) to maintain the stable number of the SSC pool. FOXC2^{-} progenies, derived from the FOXC2^{+} population, form progenitors (Figure 7Kc) to support spermatogenesis. However, it requires continuous supply from the FOXC2^{+} population and is subject to exhaustion when the supply is disrupted. In the context of regeneration conditions, the FOXC2^{+}MKI67^{-} cells can survive and set out the recovery process (Figure 7Kd). At the early stage, increasing proportion of FOXC2^{+}MKI67^{-} cells is committed to transforming into proliferative FOXC2^{+}MKI67^{+} cells, strengthening the supply to the progenitors (Figure 7Ke). At the late recovery stage, MKI67^{+}/MKI67^{-} ratio returns to the physiological level in FOXC2^{+} population (Figure 7Ka), leaving the total number of FOXC2^{+} cells stable, therefore maintaining the SSC homeostasis. However, it is necessary to perform more investigation to further improve and modify this model to gain a complete understanding of the connections between different SSC subpopulations in the testes of adult mice.

Based on our observation, FOXC2 seems nonessential for the transformation from gonocytes to SSCs in infant mice, in contrast to its requirement for adult spermatogenesis. A recent study showed that FOXC2^{+} subpopulation in the postnatal mouse testis (<5 weeks) appeared more active in proliferation than the adult counterpart (Wei et al., 2018). Such differential functionality might reflect the difference in the physical nature of spermatogenesis between developmental stages. For example, the maturity of spermatogenesis is still under development during the juvenile period with a focus on establishing and expanding the SSC pool. Therefore, it would be interesting to explore differences in individual functional contexts as well as the underlying regulatory mechanisms. Meanwhile, FOXC2, highly conserved between mice and humans with 94% identity in amino acid sequence (Miura et al., 1997), is also expressed in a subset of human adult SSCs, raising the possibility of an

evolutionarily conserved mechanism governing SSC homeostasis in humans. Further work following this direction might be of great clinical significance specifically to patients who suffer from infertility. Moreover, the developmental correlation between $FOXC2^{+}$ SSCs and other SSC subpopulations proposed previously should be revealed via biological methods such as multiple lineage tracing and live imaging. Collectively, our work here provides new insights into the investigation of adult SSCs and serves as a reference for studying the homeostasis and regeneration of other stem-cell systems.

Materials and methods

Mice

Animal experiments were approved by the Committee on Animal Care of the Institute of Basic Medical Sciences, Chinese Academy of Medical Sciences and Peking Union Medical College. The tab of animal experimental ethical inspection (No: ACUC-A01-2018-017) has been provided in supplementary file. The 8-week-old C57BL/6J wild-type mice were used for magnetic-activated cell sorting. The $Rosa26^{LSL\text{-}T/G/LSL\text{-}T/G}$ mice (stock no. 007676), $Ddx4^{Cre/+}$mice (stock no. 000692) and $EGFP^{Tg/+}$ mice (stock no. 021930) were bought from the Jackson Laboratory. The $Foxc2^{iCreERt2}$ mice and the $Foxc2^{flox/flox}$ ($Foxc2^{f/f}$) mice were constructed and bought from the Biocytogen. The $Rosa26^{LSL\text{-}DTA/+}$ mice were bought from GemPharmatech. All mice were housed and bred under specific pathogen-free conditions (temperature: 22-26°C, humidity: 40-55%, 12-h light/dark cycle) in the animal facility at the Institute of Basic Medical Sciences. DNA was isolated from the tails, and the genotypes of the mice were checked using PCR with specific primers (Materials and methods— source data 1). All mice were randomly assigned to experiments and no statistical methods were used to predetermine sample size. The person performing the experiments did not know the sample identity until after data analysis. No data were excluded from analyses and the data displayed included a minimum of three independent experiments and a minimum of three biological replicates for each independent experiment. The 8-week-old C57BL/6J WT mice were treated with busulfan (40 mg/kg) and used as recipient mice 1 month later.

Magnetic-activated cell sorting (MACS)

The testes from 8-week-old C57BL/6J wild-type mice or 4-month-old $Foxc2^{f/+}$ and $Foxc2^{f/-}$;$Ddx4^{Cre/+}$ mice (n=4) were minced and digested in the collagenase type IV (1 mg/mL, Sigma) and DNase I (500μg/mL, Sigma) at 37°C for 15 min. The cell suspension was pipetted up and down once every 5 minutes and the digestion process was stopped with DMEM (containing 10% FBS). The cell suspension was filtered through a 40-μm nylon mesh, and after centrifugation, the cells were resuspended in 8 mL PBS. The 15 mL conical centrifuge tubes were slowly overlayed with 2 mL of 70% Percoll solution, 2 mL of 30% Percoll solution, and then 2 mL of testicular cell suspension and centrifuge at 600 × g for 10 min at 4 °C without using the centrifuge brake. After centrifugation, the cells at the interface between the 70% and the 30% Percoll solution were carefully removed into the new conical centrifuge tubes, washed with PBS, and then centrifuge at 600 × g for 10 min at 4 °C. After centrifugation, the cells were resuspended in 360μL MACS buffer, added with 40μL of magnetic microbeads conjugated with anti-Thy-1 antibody (Miltenyi Biotec 130–049–101, Auburn, CA), and mixed well. Incubate the cell suspension containing Thy-1 microbeads for 20 min at 4 °C. Mix gently by tapping every 10 min. Add 20 mL of MACS buffer to the tube to dilute Thy-1 microbeads and centrifuge at 300 ×g for 10 min at 4 °C. Remove the supernatant completely and resuspend in 2 mL of MACS buffer. Place the separation columns (MS Column; Miltenyi Biotec 130-042-201) in the magnetic field of the mini MACS Separation Unit

(Miltenyi Biotec 130-142-102) and rinse with 0.5 mL of MACS buffer. Apply the cell suspension to the columns (500µL/ column). After the cell suspension has passed through the column and the column reservoir is empty, wash the column with 0.5 mL of MACS buffer three times. Remove the column from the MACS Separation Unit and elute the magnetically retained cells slowly into a 50 mL conical centrifuge tube with 1 mL of MACS buffer using the plunger supplied with the column. Centrifuge the tube containing the cells at 600 × g for 10 min at 4 °C and resuspend the cell pellet with 10 mL of MACS buffer for rinsing. Repeat this step once. After the final rinsing step, resuspend cells in 0.04% BSA and count the cell number.

Single-cell RNA-seq

The MACS-sorted THY1$^+$ cells were used for loading onto the Chromium Single Cell 3' Chip kit v2 (10x Genomics, PN-120236) according to the instructions. Cell capturing and library preparation was performed following the kit instructions of the Chromium Single Cell 3' v2 Library and Gel Bead Kit (10x Genomics, PN-120237). In brief, 5000 cells were targeted for capture, and after cDNA synthesis, 10-12 cycles were used for library amplification. The libraries were then size-selected, pooled, and sequenced on a Novaseq 6000 (Illumina). Shallow sequencing was performed to access the library quality and to adjust the subsequent sequencing depth based on the capture rate and the detected unique molecular indices (UMI).

Single-cell RNA-seq data processing

Raw sequencing reads were processed using the Cell Ranger v.3.0.1 pipeline of the 10x Genomics platform. In brief, reads from each sample were demultiplexed and aligned to the mouse mm10 genome, and UMI counts were quantified for each gene per cell to generate a gene-barcode matrix. Default parameters were used. The UMI counts were analyzed using the Seurat R Package (Stuart et al., 2019) (v.3.0.1) following the Seurat pipeline. Cells with more than 200 detected genes or less than 10% mitochondria reads were retained. Genes not detected in at least 10 cells were removed from subsequent analysis. The resulting matrix was normalized, and the most variable genes were found using Seurat's default settings, then the matrix was scaled with regression against the mitochondria reads. The top 2000 variable genes were used to perform PCA, and Jackstraw was performed using Seurat's default settings. Variation in the cells was visualized by UMAP for the top principal components. Cell types were determined using marker genes identified from the literature (Kowalczyk et al., 2015). We used the Seurat function CellCycleScoring to determine the cell cycle phase, as this program determines the relative expression of a large set of G2-M and S-phase genes. After removing the undefined cells, the spermatogonia were used for trajectory analysis, and the single-cell pseudotime trajectory was constructed with the Monocle 2 package (v2.12.0) (Qiu, Hill, et al., 2017; Qiu, Mao, et al., 2017; Trapnell et al., 2014) according to the provided documentation. The Monocle function clusterCells was used to detect cell clusters between clusters. The Seurat function FindAllMarkers with default settings was used to find DEGs upregulated in each cluster compared to the other cells. The top200 DEGs of cluster1 were used for ordering cells, and the discriminative dimensionality reduction with trees (DDRTree) method was used to reduce the data to two dimensions. The dynamic expression patterns with the spermatogonial developmental trajectory of specific genes were visualized using the Monocle function plot_genes_in_pseudotime and plot_pseudotime_heatmap. The procession data of the adult human single-cell dataset was downloaded from Gene Expression Omnibus (GEO): GSE112013 (Guo et al., 2018) and the UMI counts were analyzed using the Seurat R Package (v.3.0.1) following the Seurat pipeline with the same parameters and functions as mentioned previously. According to the known markers, the germ cells characterized was used for trajectory analysis, and the single-cell

pseudotime trajectory was constructed with the Monocle 2 package (v2.12.0) as mentioned previously.

CUT&Tag sequencing and analysis

CUT&Tag assay was performed using CUT&Tag 2.0 High-Sensitivity Kit (Novoprotein scientific Inc., Cat# N259-YH01). The detailed procedures were described in (Kaya-Okur et al., 2019; Wang et al., 2021). In brief, cells were harvested by trypsin and enriched by ConA-magnetic beads. 10,000 cells were re-suspended in 100 mL Dig-wash Buffer (20 mM HEPES pH 7.5; 150 mM NaCl; 0.5 mM Spermidine; 13 Protease inhibitor cocktail; 0.05% Digitonin) containing 2 mM EDTA and a 1:100 dilution of primary FOXC2 antibody. The primary antibody was incubated overnight at 4°C. Beads were washed in Dig-wash Buffer 3 times and incubated with secondary antibody for 1 hour at a dilution of 1:200. After incubation, the beads were washed 3 times in Dig-Hisalt Buffer (0.05% Digitonin, 20 mM HEPES, pH 7.5, 300 mM NaCl, 0.5 mM Spermidine, 13 Protease inhibitor cocktail). Cells were incubated with proteinA-Tn5 transposome at 25°C for 1 hour and washed 3 times in Dig-Hisalt buffer to remove unbound proteinA-Tn5. Next, cells were re-suspended in 100mL Tagmentation buffer (10 mM MgCl2 in Dig-Hisalt Buffer) and incubated at 37°C for 1 hour. The tagmentation was terminated by adding 2.25 mL of 0.5 M EDTA, 2.75 mL of 10% SDS and 0.5 mL of 20 mg/mL Proteinase K at 55°C for 1 hour. The DNA fragments were extracted by phenol chloroform and used for sequencing on an Illumina HiSeq instrument (Illumina NovaSeq 6000) to generate 2 × 150-bp paired-end reads following the manufacturer's instructions.

Raw reads were analyzed by removing low-quality or adaptor sequences using Trim_galore (v0.5.0) and cleaned reads were mapped to the reference genome mm10 using Bowtie2 (v2.2.5). We used MACS2 (v2.1.2) to call peaks found in different groups. Homer (v4.11.1) de novo motif discovery tool was used for finding the binding motifs of Foxc2 with the findMotifsGenome.pl command. The binding potential of candidate target genes at the binding motif was predicated using the JASPAR Scan function (binding potential >0.8). The peaks filtered by fold change more than 5 and transcription start site (TSS) less than 3000 bp were annotated by R package Chip Seeker for gene category analysis. R package Cluster profiler was used for gene function annotation such as KEGG and GO analysis.

Enrichment analyses

Gene Ontology (GO) and KEGG pathway enrichment analyses were conducted using the ClusterProfiler package (v3.12.0) (Yu et al., 2012) and the ClueGO app (v2.5.7) in Cytoscape (v3.8.1) with default settings and a p-value cut-off of 0.05. GSEA enrichment analysis was assessed using the GSEA (v4.0.2) algorithm with MSigDB (v7.0) with default settings. The signaling pathways enriched by niche-derived paracrine factors and undifferentiated SPG-derived membrane proteins in the DEGs of the four samples were characterized. Then for each niche cell type, the niche-derived signaling pathways in all four samples were crossed with the SSC-derived signaling pathways to identify the candidate signaling pathways pivotal to SSCs maintenance.

Transplantation assay

The 8-week-old C57BL/6J WT mice were treated with busulfan (40 mg/kg) and used as recipient mice 1 month later. SSCs were transplanted into the testis of recipient mice (1×10^3 cells/testis), and two months after transplantation, the testes were harvested and observed under a fluorescence microscope.

Fluorescence-activated cell sorting (FACS)

Single-cell suspensions were generated from testes or *in vitro* cultured SSCs. FACS was performed using an SH800 machine (Sony Biotechnology) to isolate the GFP^+ cells. Briefly, the GFP^+ gating area was based on the point of the fluorescence intensity axis where cells were considered as being GFP^+, set based on the background fluorescence intensity of a non-transgenic control testis cell population.

Immunofluorescence

Mouse testes were fixed in 4% Paraformaldehyde (PFA) at 4°C overnight, dehydrated, embedded in paraffin, and cut into 5-μm thick sections. The rehydrated mouse or human testis sections were subjected to antigen retrieval, blocked in 5% BSA with 0.1% Triton X-100, and incubated with primary antibody (Materials and methods—source data 1) at 4°C overnight, including the germ cell marker DDX4, undifferentiated spermatogonia markers ZBTB16, LIN28A, ECAD (Tokuda et al., 2007), GFRA1, EOMES, PAX7, progenitor marker NEUROG3, and spermatocyte marker SYCP3 (Yuan et al., 2000). After three 5-min washes in PBS, the sections were incubated with secondary antibodies (Materials and methods—source data 1) and DAPI (Sigma) at 37°C for 1 hour. After three 5-min washes in PBS, coverslips were then mounted on glass slides using anti-quencher fluorescence decay (Solarbio). Images were captured using a Zeiss 780 laser-scanning confocal microscope. Whole-mount immunofluorescence of seminiferous tubules was performed as previously described (Di Persio et al., 2017). Briefly, seminiferous tubules were disentangled from testicular biopsies and immediately fixed in 4% PFA at 4°C for 12 hours. After fixation, the seminiferous tubules were permeabilized with 0.5% Triton X-100 in PBS and treated with 5% BSA in PBS overnight at 4°C. After three 30-min washes, the seminiferous tubules were incubated with primary antibody (Materials and methods—source data 1) overnight at 4°C. After three 30-min washes, the seminiferous tubules were incubated with species-specific secondary antibodies and DAPI at 4°C for 12 hours. After three 30-min washes, the seminiferous tubules were mounted on slides with anti-quencher fluorescence decay (Solarbio) and observed with a Zeiss 780 laser-scanning confocal microscope.

RNA isolation and quantitative RT-PCR analysis

Total RNA was extracted from the testes or cultured cells using the RNeasy kit (Qiagen), reverse-transcribed using RevertAid First Strand cDNA Synthesis kit (Thermo), and processed for qRT-PCR using PowerUp SYBR Green Master Mix (Applied Biosystems) and a LightCycler 480 system (Roche) with gene-specific primers (Materials and methods—source data 1). Reactions were run in triplicate and the mRNA levels were normalized to Gapdh and quantified using the delta-delta Ct method. The values shown are mean ± s.e.m. from three biological replicates.

Tamoxifen inducible

According to a previous report for activation of iCre (M. Sharma et al., 2019), the mice were fed with TD.130859 (TAM diet) for three days. The food was formulated for 400 mg tamoxifen citrate per kg diet, which would provide ~40 mg tamoxifen per kg body weight per day.

Analyses of cyst length

The cyst length was obtained according to the previous report (Nakagawa et al., 2010). Briefly, to determine the cyst length, after immunofluorescence staining with anti-E-CAD antibody, the whole mount seminiferous tubule specimens were observed under a fluorescence microscope. The E-CAD staining coupled with staining for FOXC2 enabled us to reliably identify syncytial cysts of $FOXC2^+$ cells.

Analyses of cell density

The cell density was counted according to a previous report (Tegelenbosch & de Rooij, 1993). Briefly, the densities of the $ZBTB16^+$, $GFRA1^+$, $LIN28A^+$, or $FOXC2^+$ cells were measured on the seminiferous tubules with whole-mount staining, the numbers of which per 1000 Sertoli cells were determined.

Sperm counts

Total sperm counts were obtained according to the previous report (Roy et al., 2007). Briefly, epididymal caput and cauda were minced and incubated in prewarmed M16 medium (Sigma-Aldrich) at 37°C in air containing 5% CO_2 for 30 min to allow the sperm to swim out. Then, the sperm were diluted in water and counted using a hemocytometer.

Histology, evaluation of degenerating tubules

Testes of WT and mutant mice were fixed with PFA fixative and processed for paraffin-embedded section preparation (5 µm thick) and hematoxylin and eosin staining, according to standard procedures. The percentage of degenerating seminiferous tubules was calculated based on the cross-sections of seminiferous tubules (n > 200) that appeared on one transverse section for each testis. In normal (WT) mouse testes, four generations of germ cells, each synchronously progressing through spermatogenesis, form cellular associations of fixed composition (called seminiferous epithelial stages). In the testes of $Foxc2^{f/-};Ddx4^{Cre/+}$mice, a few tubule cross-sections lacked one or more out of the four germ cell layers, which was defined as “degenerative tubules” in this study.

Statistical analysis

All statistical analyses were performed using GraphPad Prism (v7.0). All experiments were repeated at least three times, and data for evaluated parameters are reported as mean ± s.e.m. The p-values were obtained using two-tailed unpaired Student’s t-tests or one-way ANOVA followed by Tukey test (ns represents p-value > 0.05, * represents p-value < 0.05, ** represents p-value < 0.01, *** represents p-value < 0.001, and **** represents p-value < 0.0001).

Acknowledgements

This work was supported by the National Key Research and Development Program of China grant (2022YFA0806302, 2018YFC1003500, 2019YFA0801800), CAMS Innovation Fund for Medical Sciences (CIFMS, 2021-I2M-1-019, 2017-I2M-3-009), National Natural Science Foundation of China grant (92268111, 31970794, 32000586, 31725013, 32200646), and State Key Laboratory Special fund from the Ministry of Science grant (2060204).

Materials and methods—source data 1

Excel spreadsheet with the primers and antibodies used in this study.

Data Availability

All data are available in the main text or supplementary materials. The scRNA-seq and CUT&Tag sequencing data produced in this study have been uploaded to the GEO (https://www.ncbi.nlm.nih.gov/geo) with accession codes GSE183163, GSE180729, and GSE180926. The expression of FOXC2 in adult human testis used the scRNA-seq dataset GSE112013 from previously published "The Human Testis Cell Atlas via Single-cell RNA-seq" by Jingtao Guo (https://www.ncbi.nlm.nih.gov/geo/query/acc.cgi?acc=GSE112013) (Guo et al., 2018). All of the R packages were available online and the code was used according to respective R packages documentation as described in the Methods. The MSigDB (v.7.0) used in this study is available at https://www.gsea-msigdb.org/gsea/msigdb.

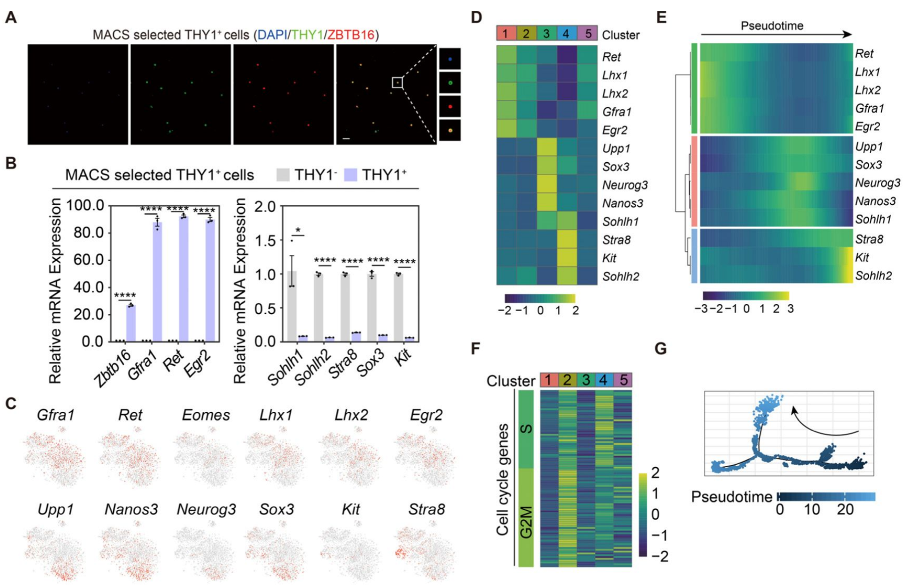

Figure 1—figure supplement 1

Validation and characterization of the MACS-sorted THY1+ uSPG from wild-type adult C57 mice.

(**A**) Immunostainings of DAPI (blue), THY1 (green), and ZBTB16 (red) in the MACS-sorted THY1+ cells (n=5). Scale bar, 50 μm. (**B**) Quantitative RT-PCR analysis of uSPG and dSPG markers expressed in the MACS-sorted THY1+ cells (n=3). Values, mean ± s.e.m.; p-values were obtained using two-tailed t-tests (ns > 0.05, *p-value < 0.05, **p-value < 0.01, ***p-value < 0.001, ****p-value < 0.0001). (**C**) Feature plots showing the expression pattern of classic SPG markers (stemness and differentiation). (**D**) Heatmap showing the expression pattern of markers for SPG in different clusters. (**E**) Expression pattern dynamics of the SPG markers with pseudotime progression. (**F**) Heatmap showing the expression pattern of markers for cell cycle phase in different clusters. (**G**) The developmental trajectory of the overall SPG, colored by pseudotime.

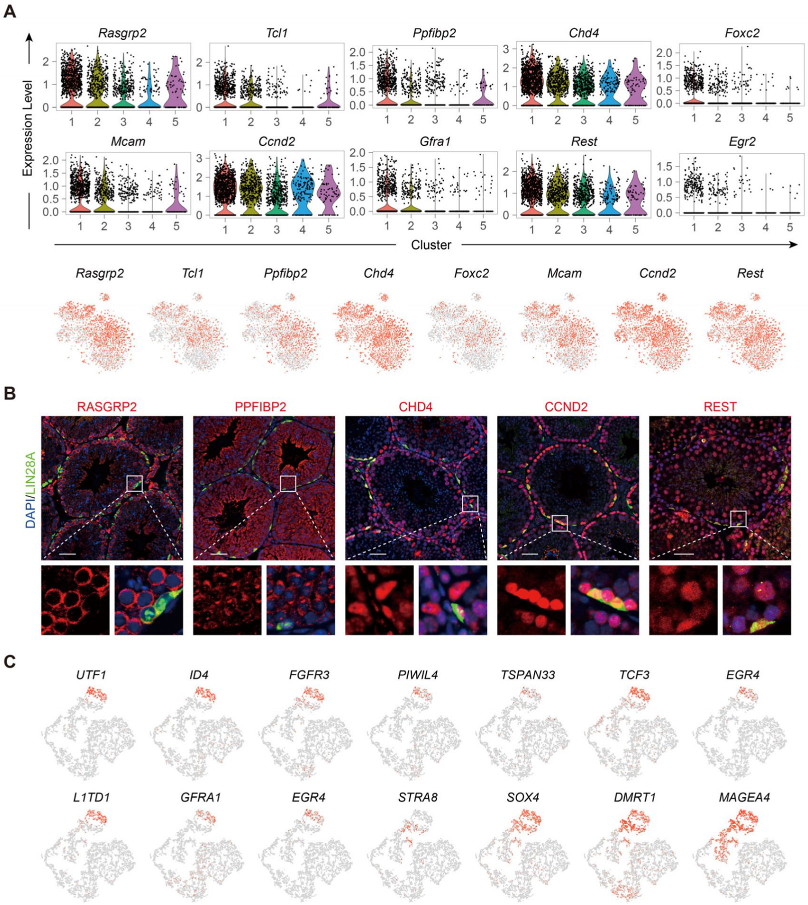

Figure 1—figure supplement 2

Expression of top10 DEGs of Cluster1 in Figure 1B and classic SSC and SPG markers in adult human germ cells.

(**A**) Feature plots and violin plots of the Top10 DEGs of Cluster1. (**B**) Immunostainings for LIN28A (red), DAPI (blue), and newly-found markers (green) in testicular paraffin sections from adult mice. Scale bar, 50 µm. (**C**) Feature plots showing the expression pattern of classic SSCs and SPG markers in adult human germ cells.

Figure 1—source data 1. Excel spreadsheet with the list of the top30 differentially expressed genes of different clusters.

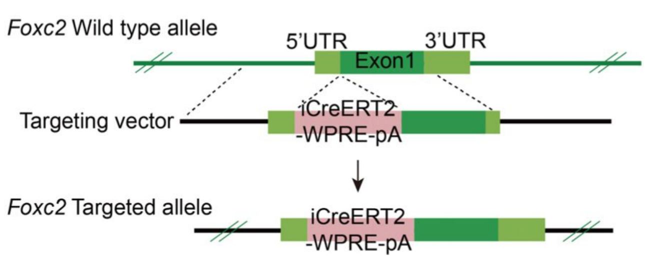

Figure 2—figure supplement 1

Construction of the *Foxc2*^{iCreERt2} mice.

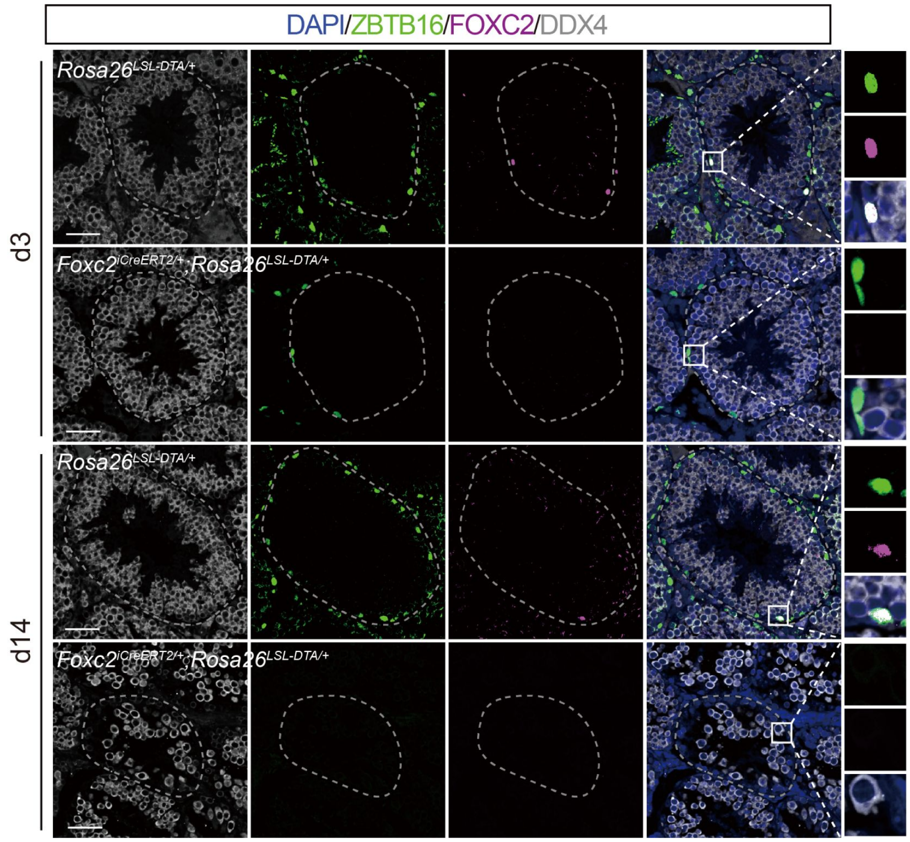

Figure 3—figure supplement 1

Depletion of uSPG pool in *Foxc2$^{iCreERT2/+}$;Rosa26$^{LSL\text{-}DTA/+}$* mice 14 days after specific ablation of FOXC2^{+} SSCs.

Immunostainings for DAPI (blue), DDX4 (white), ZBTB16 (green), and FOXC2 (magenta) at day 3 and day 14 post TAM induction in *Foxc2$^{iCreERT2/+}$;Rosa26$^{LSL\text{-}DTA/+}$* mice (scale bar, 50 µm).

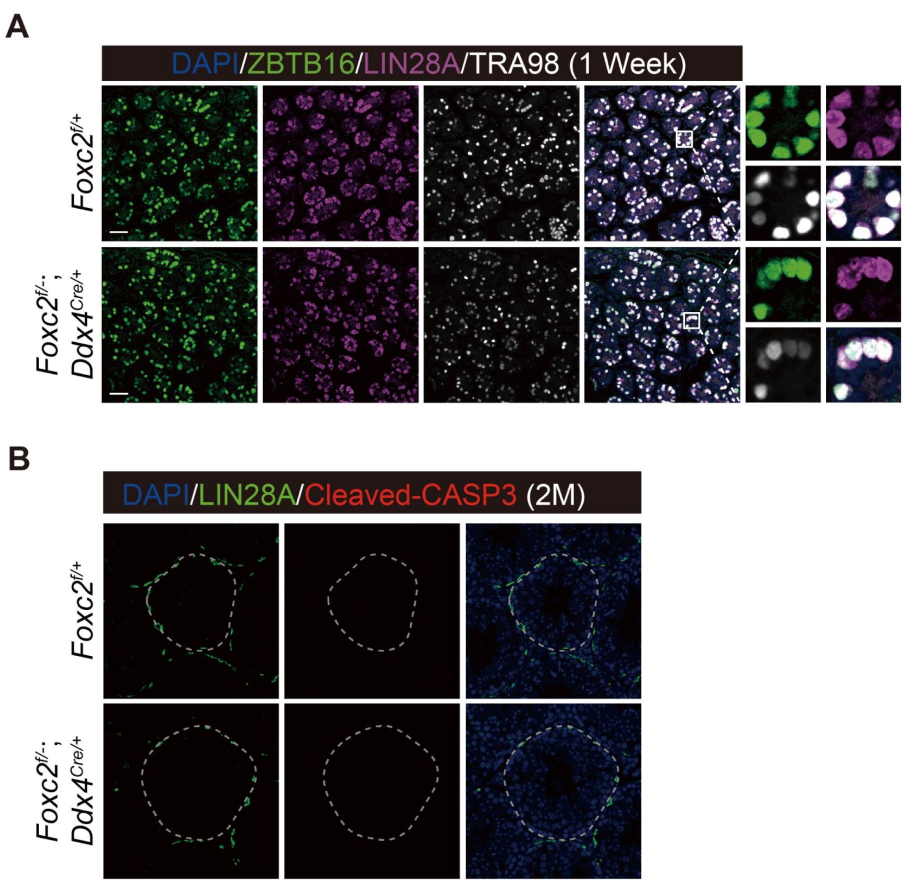

Figure 5—figure supplement 1

Phenotypic validation of the *Foxc2$^{f/-}$;Ddx4$^{Cre/+}$* mice.

(**A**) Immunostainings for DAPI (blue), ZBTB16 (green), LIN28A (magenta), and TRA98 (white) in seminiferous tubules of 1-week-old *Foxc2$^{f/+}$* and *Foxc2$^{f/-}$;Ddx4$^{Cre/+}$* mice. Scale bar, 50 µm. (**B**) Immunostainings for DAPI (blue), LIN28A (green), and Cleaved-CASP3 (red) in seminiferous of the *Foxc2$^{f/+}$* and *Foxc2$^{f/-}$;Ddx4$^{Cre/+}$* mice (2-month-old). M, month; scale bar, 50 µm.

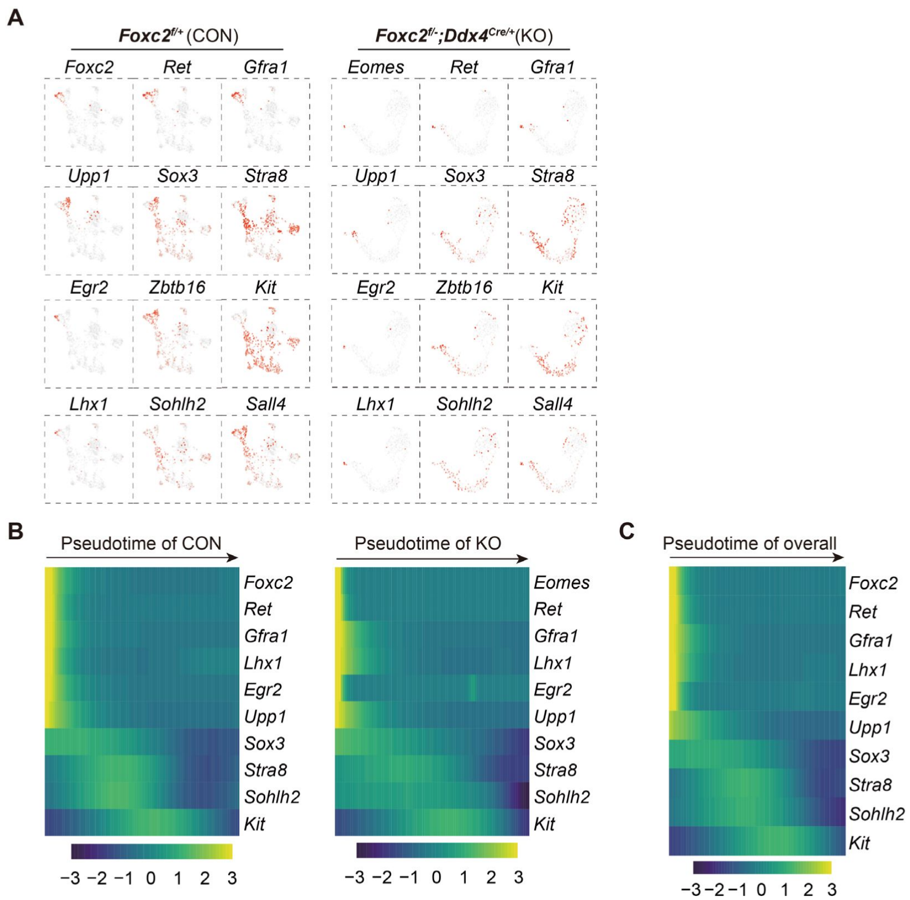

Figure 6—figure supplement 1

scRNA-seq analysis of THY1$^+$ uSPG in adult *Foxc2$^{f/+}$* and *Foxc2$^{f/-}$;Ddx4$^{Cre/+}$* mice.

(**A**) Feature plots of classic SPG markers for uSPG in adult *Foxc2$^{f/+}$* or *Foxc2$^{f/-}$;Ddx4$^{Cre/+}$* mice. (**B**) Expression dynamics of SPG markers with pseudotime progression for uSPG from *Foxc2$^{f/+}$* or *Foxc2$^{f/-}$;Ddx4$^{Cre/+}$* mice respectively. (**C**) Expression dynamics of SPG markers with pseudotime progression for overall uSPG from *Foxc2$^{f/+}$* and *Foxc2$^{f/-}$;Ddx4$^{Cre/+}$* mice.

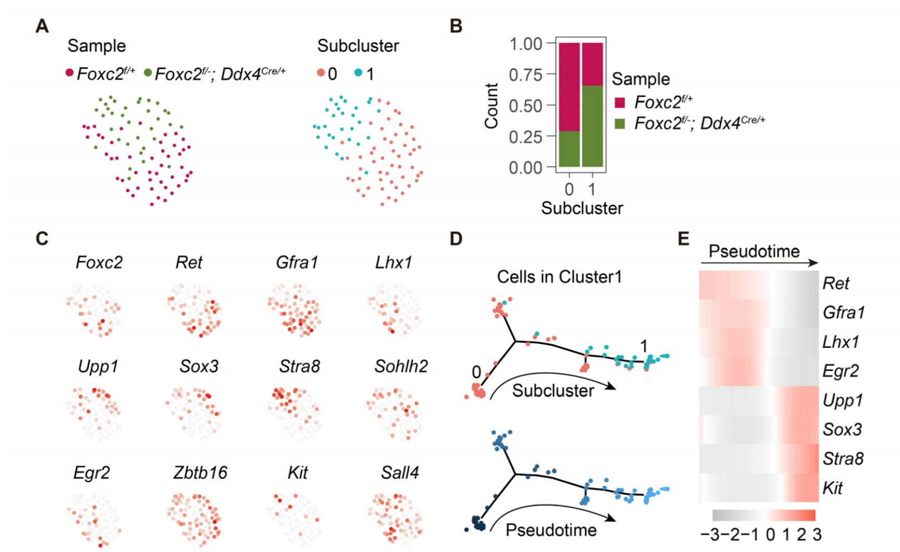

Figure 6—figure supplement 2

Re-cluster and developmental trajectory analysis of cells in Cluster1 derived from adult *Foxc2$^{f/+}$* and *Foxc2$^{f/-}$;Ddx4$^{Cre/+}$* mice.

(**A**) The t-SNE plot of the Cluster1 cells aggregated from the *Foxc2$^{f/+}$* and *Foxc2$^{f/-}$;Ddx4$^{Cre/+}$* mice colored by sample or subcluster. (**B**) The cell proportion of each sample in each subcluster. (**C**) Feature plots of SPG markers expression. (**D**) Developmental trajectory of the aggregated Cluster1 cells colored by subcluster or pseudotime. (**E**) Expression dynamics of SPG markers with pseudotime progression.

Figure 6—source data 1. Excel spreadsheet with the list of the differentially expressed genes found by scRNA-seq and enriched Gene Ontology terms.

References

Aloisio G. M. , Nakada Y. , Saatcioglu H. D. , Peña C. G. , Baker M. D. , Tarnawa E. D. , Mukherjee J. , Manjunath H. , Bugde A. , Sengupta A. L. , Amatruda J. F. , Cuevas I. , Hamra F. K. , Castrillon D. H (2014) **PAX7 expression defines germline stem cells in the adult testis** *J Clin Invest* **124**:3929–3944
https://doi.org/10.1172/jci75943

Arai F. , Suda T (2007) **Maintenance of quiescent hematopoietic stem cells in the osteoblastic niche** *Ann N Y Acad Sci* **1106**:41–53
https://doi.org/10.1196/annals.1392.005

Bahar R. , Kawamura K. , Seimiya M. , Wang Y. , Hatano M. , Okada S. , Tokuhisa T. , Watanabe T. , Tagawa M. (2002) **Growth retardation, polyploidy, and multinucleation induced by Clast3, a novel cell cycle-regulated protein** *J Biol Chem* **277**:40012–40019
https://doi.org/10.1074/jbc.M205345200

Bahuau M. , Houdayer C. , Tredano M. , Soupre V. , Couderc R. , Vazquez M. P (2002) **FOXC2 truncating mutation in distichiasis, lymphedema, and cleft palate** *Clin Genet* **62**:470–473
https://doi.org/10.1034/j.1399-0004.2002.620608.x

Bakker W. J. , Blázquez-Domingo M. , Kolbus A. , Besooyen J. , Steinlein P. , Beug H. , Coffer P. J. , Löwenberg B. , von Lindern M. , van Dijk T. B. (2004) **FoxO3a regulates erythroid differentiation and induces BTG1, an activator of protein arginine methyl transferase 1** *J Cell Biol* **164**:175–184
https://doi.org/10.1083/jcb.200307056

Buaas F. W. , Kirsh A. L. , Sharma M. , McLean D. J. , Morris J. L. , Griswold M. D. , de Rooij D. G. , Braun R. E. (2004) **Plzf is required in adult male germ cells for stem cell self-renewal** *Nat Genet* **36**:647–652
https://doi.org/10.1038/ng1366

Cheung T. H. , Rando T. A (2013) **Molecular regulation of stem cell quiescence** *Nat Rev Mol Cell Biol* **14**:329–340
https://doi.org/10.1038/nrm3591

Clermont Y (1966) **Renewal of spermatogonia in man** *Am J Anat* **118**:509–524
https://doi.org/10.1002/aja.1001180211

Clermont Y (1966) **Spermatogenesis in man. A study of the spermatogonial population** *Fertil Steril* **17**:705–721

Clermont Y (1969) **Two classes of spermatogonial stem cells in the monkey (Cercopithecus aethiops)** *Am J Anat* **126**:57–71
https://doi.org/10.1002/aja.1001260106

Costoya J. A. , Hobbs R. M. , Barna M. , Cattoretti G. , Manova K. , Sukhwani M. , Orwig K. E. , Wolgemuth D. J. , Pandolfi P. P (2004) **Essential role of Plzf in maintenance of spermatogonial stem cells** *Nat Genet* **36**:653–659
https://doi.org/10.1038/ng1367

Davis K. E. , Moldes M. , Farmer S. R (2004) **The forkhead transcription factor FoxC2 inhibits white adipocyte differentiation** *J Biol Chem* **279**:42453–42461
https://doi.org/10.1074/jbc.M402197200

Di Persio S. , Saracino R. , Fera S. , Muciaccia B. , Esposito V. , Boitani C. , Berloco B. P. , Nudo F. , Spadetta G. , Stefanini M. , de Rooij D. G. , Vicini E. (2017) **Spermatogonial kinetics in humans** *Development* **144**:3430–3439
https://doi.org/10.1242/dev.150284

Ehmcke J. , Schlatt S (2006) **A revised model for spermatogonial expansion in man: lessons from non-human primates** *Reproduction* **132**:673–680
https://doi.org/10.1530/rep.1.01081

Ehmcke J. , Wistuba J. , Schlatt S (2006) **Spermatogonial stem cells: questions, models and perspectives** *Hum Reprod Update* **12**:275–282
https://doi.org/10.1093/humupd/dmk001

Faisal I. , Cisneros-Montalvo S. , Hamer G. , Tuominen M. M. , Laurila P. P. , Tumiati M. , Jauhiainen M. , Kotaja N. , Toppari J. , Mäkelä J. A. , Kauppi L. (2019) **Transcription Factor USF1 Is Required for Maintenance of Germline Stem Cells in Male Mice** *Endocrinology* **160**:1119–1136
https://doi.org/10.1210/en.2018-01088

Gallardo T. , Shirley L. , John G. B. , Castrillon D. H (2007) **Generation of a germ cell-specific mouse transgenic Cre line, Vasa-Cre** *Genesis* **45**:413–417
https://doi.org/10.1002/dvg.20310

Gaudet P. , Livstone M. S. , Lewis S. E. , Thomas P. D (2011) **Phylogenetic-based propagation of functional annotations within the Gene Ontology consortium** *Brief Bioinform* **12**:449–462
https://doi.org/10.1093/bib/bbr042

Georgescu M. M. , Cote G. , Agarwal N. K. , White C. L (2014) **NHERF1/EBP50 controls morphogenesis of 3D colonic glands by stabilizing PTEN and ezrin-radixin-moesin proteins at the apical membrane** *Neoplasia* **16**:365–374
https://doi.org/10.1016/j.neo.2014.04.004

Guo J. , Grow E. J. , Mlcochova H. , Maher G. J. , Lindskog C. , Nie X. , Guo Y. , Takei Y. , Yun J. , Cai L. , Kim R. , Carrell D. T. , Goriely A. , Hotaling J. M. , Cairns B. R (2018) **The adult human testis transcriptional cell atlas** *Cell Res* **28**:1141–1157
https://doi.org/10.1038/s41422-018-0099-2

Guo R. , Yu Z. , Guan J. , Ge Y. , Ma J. , Li S. , Wang S. , Xue S. , Han D (2004) **Stage-specific and tissue-specific expression characteristics of differentially expressed genes during mouse spermatogenesis** *Mol Reprod Dev* **67**:264–272
https://doi.org/10.1002/mrd.20026

Hammoud S. S. , Low D. H. , Yi C. , Carrell D. T. , Guccione E. , Cairns B. R (2014) **Chromatin and transcription transitions of mammalian adult germline stem cells and spermatogenesis** *Cell Stem Cell* **15**:239–253
https://doi.org/10.1016/j.stem.2014.04.006

Hara K. , Nakagawa T. , Enomoto H. , Suzuki M. , Yamamoto M. , Simons B. D. , Yoshida S (2014) **Mouse spermatogenic stem cells continually interconvert between equipotent singly isolated and syncytial states** *Cell Stem Cell* **14**:658–672
https://doi.org/10.1016/j.stem.2014.01.019

Helsel A. R. , Yang Q. E. , Oatley M. J. , Lord T. , Sablitzky F. , Oatley J. M (2017) **ID4 levels dictate the stem cell state in mouse spermatogonia** *Development* **144**:624–634
https://doi.org/10.1242/dev.146928

Hermann B. P. , Cheng K. , Singh A. , Roa-De La Cruz L. , Mutoji K. N. , Chen I. C. , Gildersleeve H. , Lehle J. D. , Mayo M. , Westernströer B. , Law N. C. , Oatley M. J. , Velte E. K. , Niedenberger B. A. , Fritze D. , Silber S. , Geyer C. B. , Oatley J. M. , McCarrey J. R. (2018) **The Mammalian Spermatogenesis Single-Cell Transcriptome, from Spermatogonial Stem Cells to Spermatids** *Cell Rep* **25**:1650–1667
https://doi.org/10.1016/j.celrep.2018.10.026

Jijiwa M. , Kawai K. , Fukihara J. , Nakamura A. , Hasegawa M. , Suzuki C. , Sato T. , Enomoto A. , Asai N. , Murakumo Y. , Takahashi M (2008) **GDNF-mediated signaling via RET tyrosine 1062 is essential for maintenance of spermatogonial stem cells** *Genes Cells* **13**:365–374
https://doi.org/10.1111/j.1365-2443.2008.01171.x

Kanatsu-Shinohara M. , Morimoto H. , Shinohara T. (2012) **Enrichment of mouse spermatogonial stem cells by melanoma cell adhesion molecule expression** *Biol Reprod* **87**
https://doi.org/10.1095/biolreprod.112.103861

Kaya-Okur H. S. , Janssens D. H. , Henikoff J. G. , Ahmad K. , Henikoff S. (2020) **Efficient low-cost chromatin profiling with CUT&Tag** *Nat Protoc* **15**:3264–3283
https://doi.org/10.1038/s41596-020-0373-x

Kaya-Okur H. S. , Wu S. J. , Codomo C. A. , Pledger E. S. , Bryson T. D. , Henikoff J. G. , Ahmad K. , Henikoff S. (2019) **CUT&Tag for efficient epigenomic profiling of small samples and single cells** *Nat Commun* **10**
https://doi.org/10.1038/s41467-019-09982-5

Knudson C. M. , Korsmeyer S. J (1997) **Bcl-2 and Bax function independently to regulate cell death** *Nat Genet* **16**:358–363
https://doi.org/10.1038/ng0897-358

Kowalczyk M. S. , Tirosh I. , Heckl D. , Rao T. N. , Dixit A. , Haas B. J. , Schneider R. K. , Wagers A. J. , Ebert B. L. , Regev A (2015) **Single-cell RNA-seq reveals changes in cell cycle and differentiation programs upon aging of hematopoietic stem cells** *Genome Res* **25**:1860–1872
https://doi.org/10.1101/gr.192237.115

Kubota H. , Avarbock M. R. , Brinster R. L (2004) **Culture conditions and single growth factors affect fate determination of mouse spermatogonial stem cells** *Biol Reprod* **71**:722–731
https://doi.org/10.1095/biolreprod.104.029207

Kume T. , Jiang H. , Topczewska J. M. , Hogan B. L (2001) **The murine winged helix transcription factors, Foxc1 and Foxc2, are both required for cardiovascular development and somitogenesis** *Genes Dev* **15**:2470–2482
https://doi.org/10.1101/gad.907301

La H. M. , Hobbs R. M (2019) **Mechanisms regulating mammalian spermatogenesis and fertility recovery following germ cell depletion** *Cell Mol Life Sci* **76**:4071–4102
https://doi.org/10.1007/s00018-019-03201-6

La H. M. , Mäkelä J. A. , Chan A. L. , Rossello F. J. , Nefzger C. M. , Legrand J. M. D. , De Seram M. , Polo J. M. , Hobbs R. M. (2018) **Identification of dynamic undifferentiated cell states within the male germline** *Nat Commun* **9**
https://doi.org/10.1038/s41467-018-04827-z

Li H. , Liang Z. , Yang J. , Wang D. , Wang H. , Zhu M. , Geng B. , Xu E. Y (2019) **DAZL is a master translational regulator of murine spermatogenesis** *Natl Sci Rev* **6**:455–468
https://doi.org/10.1093/nsr/nwy163

Liao H. F. , Chen W. S. , Chen Y. H. , Kao T. H. , Tseng Y. T. , Lee C. Y. , Chiu Y. C. , Lee P. L. , Lin Q. J. , Ching Y. H. , Hata K. , Cheng W. T. , Tsai M. H. , Sasaki H. , Ho H. N. , Wu S. C. , Huang Y. H. , Yen P. , Lin S. P (2014) **DNMT3L promotes quiescence in postnatal spermatogonial progenitor cells** *Development* **141**:2402–2413
https://doi.org/10.1242/dev.105130

Miura N. , Iida K. , Kakinuma H. , Yang X. L. , Sugiyama T (1997) **Isolation of the mouse (MFH-1) and human (FKHL 14) mesenchyme fork head-1 genes reveals conservation of their gene and protein structures** *Genomics* **41**:489–492
https://doi.org/10.1006/geno.1997.4695

Motojima M. , Tanimoto S. , Ohtsuka M. , Matsusaka T. , Kume T. , Abe K (2016) **Characterization of Kidney and Skeleton Phenotypes of Mice Double Heterozygous for Foxc1 and Foxc2** *Cells Tissues Organs* **201**:380–389
https://doi.org/10.1159/000445027

Nakagawa T. , Jörg D. J. , Watanabe H. , Mizuno S. , Han S. , Ikeda T. , Omatsu Y. , Nishimura K. , Fujita M. , Takahashi S. , Kondoh G. , Simons B. D. , Yoshida S. , Nagasawa T (2021) **A multistate stem cell dynamics maintains homeostasis in mouse spermatogenesis** *Cell Rep* **37**
https://doi.org/10.1016/j.celrep.2021.109875

Nakagawa T. , Nabeshima Y. , Yoshida S (2007) **Functional identification of the actual and potential stem cell compartments in mouse spermatogenesis** *Dev Cell* **12**:195–206
https://doi.org/10.1016/j.devcel.2007.01.002

Nakagawa T. , Sharma M. , Nabeshima Y. , Braun R. E. , Yoshida S (2010) **Functional hierarchy and reversibility within the murine spermatogenic stem cell compartment** *Science* **328**:62–67
https://doi.org/10.1126/science.1182868

Nitiss J. L (2009) **DNA topoisomerase II and its growing repertoire of biological functions** *Nat Rev Cancer* **9**:327–337
https://doi.org/10.1038/nrc2608

Oatley J. M. , Avarbock M. R. , Brinster R. L (2007) **Glial cell line-derived neurotrophic factor regulation of genes essential for self-renewal of mouse spermatogonial stem cells is dependent on Src family kinase signaling** *J Biol Chem* **282**:25842–25851
https://doi.org/10.1074/jbc.M703474200

Qiu X. , Hill A. , Packer J. , Lin D. , Ma Y. A. , Trapnell C (2017) **Single-cell mRNA quantification and differential analysis with Census** *Nat Methods* **14**:309–315
https://doi.org/10.1038/nmeth.4150

Qiu X. , Mao Q. , Tang Y. , Wang L. , Chawla R. , Pliner H. A. , Trapnell C (2017) **Reversed graph embedding resolves complex single-cell trajectories** *Nat Methods* **14**:979–982
https://doi.org/10.1038/nmeth.4402

Raman M. , Earnest S. , Zhang K. , Zhao Y. , Cobb M. H (2007) **TAO kinases mediate activation of p38 in response to DNA damage** *Embo j* **26**:2005–2014
https://doi.org/10.1038/sj.emboj.7601668

Relaix F. , Zammit P. S (2012) **Satellite cells are essential for skeletal muscle regeneration: the cell on the edge returns centre stage** *Development* **139**:2845–2856
https://doi.org/10.1242/dev.069088

Rodgers J. T. , King K. Y. , Brett J. O. , Cromie M. J. , Charville G. W. , Maguire K. K. , Brunson C. , Mastey N. , Liu L. , Tsai C. R. , Goodell M. A. , Rando T. A (2014) **mTORC1 controls the adaptive transition of quiescent stem cells from G0 to G(Alert)** *Nature* **510**:393–396
https://doi.org/10.1038/nature13255

Roy A. , Lin Y. N. , Agno J. E. , DeMayo F. J. , Matzuk M. M (2007) **Absence of tektin 4 causes asthenozoospermia and subfertility in male mice** *Faseb j* **21**:1013–1025
https://doi.org/10.1096/fj.06-7035com

Sabine A. , Bovay E. , Demir C. S. , Kimura W. , Jaquet M. , Agalarov Y. , Zangger N. , Scallan J. P. , Graber W. , Gulpinar E. , Kwak B. R. , Mäkinen T. , Martinez-Corral I. , Ortega S. , Delorenzi M. , Kiefer F. , Davis M. J. , Djonov V. , Miura N. , Petrova T. V. (2015) **FOXC2 and fluid shear stress stabilize postnatal lymphatic vasculature** *J Clin Invest* **125**:3861–3877
https://doi.org/10.1172/jci80454

Sada A. , Suzuki A. , Suzuki H. , Saga Y (2009) **The RNA-binding protein NANOS2 is required to maintain murine spermatogonial stem cells** *Science* **325**:1394–1398
https://doi.org/10.1126/science.1172645

Sasman A. , Nassano-Miller C. , Shim K. S. , Koo H. Y. , Liu T. , Schultz K. M. , Millay M. , Nanano A. , Kang M. , Suzuki T. , Kume T. (2012) **Generation of conditional alleles for Foxc1 and Foxc2 in mice** *Genesis* **50**:766–774
https://doi.org/10.1002/dvg.22036

Sharma M. , Srivastava A. , Fairfield H. E. , Bergstrom D. , Flynn W. F. , Braun R. E (2019) **Identification of EOMES-expressing spermatogonial stem cells and their regulation by PLZF** *Elife* **8**
https://doi.org/10.7554/eLife.43352

Sharma S. , Wistuba J. , Pock T. , Schlatt S. , Neuhaus N (2019) **Spermatogonial stem cells: updates from specification to clinical relevance** *Hum Reprod Update* **25**:275–297
https://doi.org/10.1093/humupd/dmz006

Stuart T. , Butler A. , Hoffman P. , Hafemeister C. , Papalexi E. , Mauck W. M , Hao Y. , Stoeckius M. , Smibert P. , Satija R. (2019) **Comprehensive Integration of Single-Cell Data** *Cell* **177**:1888–1902
https://doi.org/10.1016/j.cell.2019.05.031

Suzuki S. , McCarrey J. R. , Hermann B. P (2021) **An mTORC1-dependent switch orchestrates the transition between mouse spermatogonial stem cells and clones of progenitor spermatogonia** *Cell Rep* **34**
https://doi.org/10.1016/j.celrep.2021.108752

Tan K. , Wilkinson M. F (2019) **Human Spermatogonial Stem Cells Scrutinized under the Single-Cell Magnifying Glass** *Cell Stem Cell* **24**:201–203
https://doi.org/10.1016/j.stem.2019.01.010

Tegelenbosch R. A. , de Rooij D. G. (1993) **A quantitative study of spermatogonial multiplication and stem cell renewal in the C3H/101 F1 hybrid mouse** *Mutat Res* **290**:193–200
https://doi.org/10.1016/0027-5107(93)90159-d

Tokuda M. , Kadokawa Y. , Kurahashi H. , Marunouchi T (2007) **CDH1 is a specific marker for undifferentiated spermatogonia in mouse testes** *Biol Reprod* **76**:130–141
https://doi.org/10.1095/biolreprod.106.053181

Tokue M. , Ikami K. , Mizuno S. , Takagi C. , Miyagi A. , Takada R. , Noda C. , Kitadate Y. , Hara K. , Mizuguchi H. , Sato T. , Taketo M. M. , Sugiyama F. , Ogawa T. , Kobayashi S. , Ueno N. , Takahashi S. , Takada S. , Yoshida S (2017) **SHISA6 Confers Resistance to Differentiation-Promoting Wnt/β-Catenin Signaling in Mouse Spermatogenic Stem Cells** *Stem Cell Reports* **8**:561–575
https://doi.org/10.1016/j.stemcr.2017.01.006

Toyooka Y. , Tsunekawa N. , Takahashi Y. , Matsui Y. , Satoh M. , Noce T (2000) **Expression and intracellular localization of mouse Vasa-homologue protein during germ cell development** *Mech Dev* **93**:139–149
https://doi.org/10.1016/s0925-4773(00)00283-5

Trapnell C. , Cacchiarelli D. , Grimsby J. , Pokharel P. , Li S. , Morse M. , Lennon N. J. , Livak K. J. , Mikkelsen T. S. , Rinn J. L (2014) **The dynamics and regulators of cell fate decisions are revealed by pseudotemporal ordering of single cells** *Nat Biotechnol* **32**:381–386
https://doi.org/10.1038/nbt.2859

van Oosten M. , Stout G. J. , Backendorf C. , Rebel H. , de Wind N. , Darroudi F. , van Kranen H. J. , de Gruijl F. R. , Mullenders L. H. (2005) **Mismatch repair protein Msh2 contributes to UVB-induced cell cycle arrest in epidermal and cultured mouse keratinocytes** *DNA Repair (Amst)* **4**:81–89
https://doi.org/10.1016/j.dnarep.2004.08.008

van Velthoven C. T. J. , Rando T. A. (2019) **Stem Cell Quiescence: Dynamism, Restraint, and Cellular Idling** *Cell Stem Cell* **24**:213–225
https://doi.org/10.1016/j.stem.2019.01.001

Wang D. , Cai C. , Dong X. , Yu Q. C. , Zhang X. O. , Yang L. , Zeng Y. A (2015) **Identification of multipotent mammary stem cells by protein C receptor expression** *Nature* **517**:81–84
https://doi.org/10.1038/nature13851

Wang M. , Liu X. , Chang G. , Chen Y. , An G. , Yan L. , Gao S. , Xu Y. , Cui Y. , Dong J. , Chen Y. , Fan X. , Hu Y. , Song K. , Zhu X. , Gao Y. , Yao Z. , Bian S. , Hou Y. , Qiao J. (2018) **Single-Cell RNA Sequencing Analysis Reveals Sequential Cell Fate Transition during Human Spermatogenesis** *Cell Stem Cell* **23**:599–614
https://doi.org/10.1016/j.stem.2018.08.007

Wang X. , Liu C. , Zhang S. , Yan H. , Zhang L. , Jiang A. , Liu Y. , Feng Y. , Li D. , Guo Y. , Hu X. , Lin Y. , Bu P. , Li D (2021) **N(6)-methyladenosine modification of MALAT1 promotes metastasis via reshaping nuclear speckles** *Dev Cell* **56**:702–715
https://doi.org/10.1016/j.devcel.2021.01.015

Weaver B. A. , Bonday Z. Q. , Putkey F. R. , Kops G. J. , Silk A. D. , Cleveland D. W (2003) **Centromere-associated protein-E is essential for the mammalian mitotic checkpoint to prevent aneuploidy due to single chromosome loss** *J Cell Biol* **162**:551–563
https://doi.org/10.1083/jcb.200303167

Wei C. , Lin H. , Cui S (2018) **The Forkhead Transcription Factor FOXC2 Is Required for Maintaining Murine Spermatogonial Stem Cells** *Stem Cells Dev* **27**:624–636
https://doi.org/10.1089/scd.2017.0233

Yi X. , Hong M. , Gui B. , Chen Z. , Li L. , Xie G. , Liang J. , Wang X. , Shang Y (2012) **RNA processing and modification protein, carbon catabolite repression 4 (Ccr4), arrests the cell cycle through p21-dependent and p53-independent pathway** *J Biol Chem* **287**:21045–21057
https://doi.org/10.1074/jbc.M112.355321

Yuan L. , Liu J. G. , Zhao J. , Brundell E. , Daneholt B. , Höög C (2000) **The murine SCP3 gene is required for synaptonemal complex assembly, chromosome synapsis, and male fertility** *Mol Cell* **5**:73–83
https://doi.org/10.1016/s1097-2765(00)80404-9

Zheng K. , Wu X. , Kaestner K. H. , Wang P. J (2009) **The pluripotency factor LIN28 marks undifferentiated spermatogonia in mouse** *BMC Dev Biol* **9**
https://doi.org/10.1186/1471-213x-9-38

Author information

Zhipeng Wang
Department of Biochemistry and Molecular Biology, State Key Laboratory of Medical Molecular Biology, Institute of Basic Medical Sciences Chinese Academy of Medical Sciences, School of Basic Medicine Peking Union Medical College; Beijing, 100005, China

Cheng Jin
Department of Biochemistry and Molecular Biology, State Key Laboratory of Medical Molecular Biology, Institute of Basic Medical Sciences Chinese Academy of Medical Sciences, School of Basic Medicine Peking Union Medical College; Beijing, 100005, China

Pengyu Li
Department of Biochemistry and Molecular Biology, State Key Laboratory of Medical Molecular Biology, Institute of Basic Medical Sciences Chinese Academy of Medical Sciences, School of Basic Medicine Peking Union Medical College; Beijing, 100005, China

Yiran Li
Department of Biochemistry and Molecular Biology, State Key Laboratory of Medical Molecular Biology, Institute of Basic Medical Sciences Chinese Academy of Medical Sciences, School of Basic Medicine Peking Union Medical College; Beijing, 100005, China

Jielin Tang
Department of Biochemistry and Molecular Biology, State Key Laboratory of Medical Molecular Biology, Institute of Basic Medical Sciences Chinese Academy of Medical Sciences, School of Basic Medicine Peking Union Medical College; Beijing, 100005, China

Zhixin Yu
Department of Biochemistry and Molecular Biology, State Key Laboratory of Medical Molecular Biology, Institute of Basic Medical Sciences Chinese Academy of Medical Sciences, School of Basic Medicine Peking Union Medical College; Beijing, 100005, China

Tao Jiao
Department of Biochemistry and Molecular Biology, State Key Laboratory of Medical Molecular Biology, Institute of Basic Medical Sciences Chinese Academy of Medical Sciences, School of Basic Medicine Peking Union Medical College; Beijing, 100005, China

Jinhuan Ou
Department of Biochemistry and Molecular Biology, State Key Laboratory of Medical Molecular Biology, Institute of Basic Medical Sciences Chinese Academy of Medical Sciences, School of Basic Medicine Peking Union Medical College; Beijing, 100005, China

Han Wang
Department of Biochemistry and Molecular Biology, State Key Laboratory of Medical Molecular Biology, Institute of Basic Medical Sciences Chinese Academy of Medical Sciences, School of Basic Medicine Peking Union Medical College; Beijing, 100005, China

Dingfeng Zou
Department of Biochemistry and Molecular Biology, State Key Laboratory of Medical Molecular Biology, Institute of Basic Medical Sciences Chinese Academy of Medical Sciences, School of Basic Medicine Peking Union Medical College; Beijing, 100005, China

Mengzhen Li
Department of Biochemistry and Molecular Biology, State Key Laboratory of Medical Molecular Biology, Institute of Basic Medical Sciences Chinese Academy of Medical Sciences, School of Basic Medicine Peking Union Medical College; Beijing, 100005, China

Xinyu Mang
Department of Biochemistry and Molecular Biology, State Key Laboratory of Medical Molecular Biology, Institute of Basic Medical Sciences Chinese Academy of Medical Sciences, School of Basic Medicine Peking Union Medical College; Beijing, 100005, China

Jun Liu
Department of Biochemistry and Molecular Biology, State Key Laboratory of Medical Molecular Biology, Institute of Basic Medical Sciences Chinese Academy of Medical Sciences, School of Basic Medicine Peking Union Medical College; Beijing, 100005, China

Yan Lu
Department of Biochemistry and Molecular Biology, State Key Laboratory of Medical Molecular Biology, Institute of Basic Medical Sciences Chinese Academy of Medical Sciences, School of Basic Medicine Peking Union Medical College; Beijing, 100005, China

Kai Li
Department of Biochemistry and Molecular Biology, State Key Laboratory of Medical Molecular Biology, Institute of Basic Medical Sciences Chinese Academy of Medical Sciences, School of Basic Medicine Peking Union Medical College; Beijing, 100005, China

Ning Zhang
MRC Protein Phosphorylation and Ubiquitylation Unit, School of Life Sciences, University of Dundee; Dundee, DD1 5EH, UK

Jia Yu
Department of Biochemistry and Molecular Biology, State Key Laboratory of Medical Molecular Biology, Institute of Basic Medical Sciences Chinese Academy of Medical Sciences, School of Basic Medicine Peking Union Medical College; Beijing, 100005, China

Shiying Miao
Department of Biochemistry and Molecular Biology, State Key Laboratory of Medical Molecular Biology, Institute of Basic Medical Sciences Chinese Academy of Medical Sciences, School of Basic Medicine Peking Union Medical College; Beijing, 100005, China

Linfang Wang
Department of Biochemistry and Molecular Biology, State Key Laboratory of Medical Molecular Biology, Institute of Basic Medical Sciences Chinese Academy of Medical Sciences, School of Basic Medicine Peking Union Medical College; Beijing, 100005, China

Wei Song
Department of Biochemistry and Molecular Biology, State Key Laboratory of Medical Molecular Biology, Institute of Basic Medical Sciences Chinese Academy of Medical Sciences, School of Basic Medicine Peking Union Medical College; Beijing, 100005, China

For correspondence: songwei@ibms.pumc.edu.cn

ORCID iD: 0000-0002-8395-9991

Editors

Reviewing Editor
Wei Yan
University of California, Los Angeles, United States of America

Senior Editor
Diane Harper
University of Michigan, United States of America

Reviewer #1 (Public Review):

The expression and localization of Foxc2 strongly suggest that its role is mainly confined to As undifferentiated spermatogonia (uSPGs). Lineage tracing demonstrated that all germ cells were derived from the FOXC2+ uSPGs. Specific ablation of the FOXC2+ uSPGs led to the depletion of all uSPG populations. Full spermatogenesis can be achieved through the transplantation of Foxc2+ uSPGs. Male germ cell-specific ablation of Foxc2 caused Sertoli-only testes in mice. CUT&Tag sequencing revealed that FOXC2 regulates the factors that inhibit the mitotic cell cycle, consistent with its potential role in maintaining a quiescent state in As spermatogonia. These data made the authors conclude that the FOXC2+ uSPG may be the true SSCs, essential for maintaining spermatogenesis. The conclusion is supported by the data presented.

Reviewer #2 (Public Review):

The authors found FOXC2 is mainly expressed in As of mouse undifferentiated spermatogonia (uSPG). About 60% of As uSPG were FOXC2+ MKI67-, indicating that FOXC2 uSPG were quiescent. Similar spermatogonia (ZBTB16+ FOXC2+ MKI67-) were also found in human testis.

The lineage tracing experiment using Foxc2CRE/+;R26T/Gf/f mice demonstrated that all germ cells were derived from the FOXC2+ uSPG. Furthermore, specific ablation of the FOXC2+ uSPGs using Foxc2Cre/+;R26DTA/+ mice resulted in the depletion of all uSPG population. In the regenerative condition created by busulfan injection, all FOXC2+ uSPG survived and began to proliferate at around 30 days after busulfan injection. The survived FOXC2+ uSPGs generated all germ cells eventually. To examine the role of FOXC2 in the adult testis, spermatogenesis of Foxc2f/-;Ddx4-cre mice was analyzed. From a 2-month-old, the

degenerative seminiferous tubules were increased and became Sertoli cell-only seminiferous tubules, indicating FOXC2 is required to maintain normal spermatogenesis in adult testes. To get insight into the role of FOXC2 in the uSPG, CUT&Tag sequencing was performed in sorted FOXC2+ uSPG from Foxc2CRE/+;R26T/Gf/f mice 3 days after TAM diet feeding. The results showed some unique biological processes, including negative regulation of the mitotic cell cycle, were enriched, suggesting the FOXC2 maintains a quiescent state in spermatogonia.

Lineage tracing experiments using transgenic mice of the TAM-inducing system was well-designed and demonstrated interesting results. Based on all data presented, the authors concluded that the FOXC2+ uSPG are primitive SSCs, an indispensable subpopulation to maintain adult spermatogenesis. The conclusion of the mouse study is supported by the data presented.

Reviewer #3 (Public Review):

By popular single-cell RNA-seq, the authors identified FOXC2 as an undifferentiated spermatogonia-specific expressed gene. The FOXC2+-SSCs can sufficiently initiate and sustain spermatogenesis, the ablation of this subgroup results in the depletion of the uSPG pool. The authors provide further evidence to show that this gene is essential for SSCs maintenance by negatively regulating the cell cycle in adult mice, thus well-established FOXC2 as a key regulator of SSCs quiescent state.

The experiments are well-designed and conducted, the overall conclusions are convincing. This work will be of interest to stem cell and reproductive biologists.

Author Response:

The following is the authors’ response to the original reviews.

> ### *Reviewer #1 (Public Review):*

> *The expression and localization of Foxc2 strongly suggest that its role is mainly confined to As undifferentiated spermatogonia (uSPGs). Lineage tracing demonstrated that all germ cells were derived from the FOXC2+ uSPGs. Specific ablation of the FOXC2+ uSPGs led to the depletion of all uSPG populations. Full spermatogenesis can be achieved through the transplantation of Foxc2+ uSPGs. Male germ cell-specific ablation of Foxc2 caused Sertoli-only testes in mice. CUT&Tag sequencing revealed that FOXC2 regulates the factors that inhibit the mitotic cell cycle, consistent with its potential role in maintaining a quiescent state in As spermatogonia. These data made the authors conclude that the FOXC2+ uSPG may be the true SSCs, essential for maintaining spermatogenesis. The conclusion is largely supported by the data presented, but two concerns should be addressed: 1) terminology used is confusing: primitive SSCs, primitive uSPGs, transit amplifying SSCs... 2) the GFP+ cells used for germ cell transplantation should be better controlled using THY1+ cells.*

Thanks for your good comments. According to your suggestions, we have addressed your two concerns as follows:

1> Overall our work suggest that FOXC2+ SSCs are a subpopulation of SSCs in a quiescent state, thus we have replaced the term ‘primitive’ with ‘quiescent’ in the revised manuscript. In general, ‘transient amplifying SSCs’ is considered to be ‘progenitors’, thus we have replaced ‘transient amplifying SSCs’ with ‘progenitors’ in the revised manuscript.

2> The transplantation experiment was conducted using MACS-sorted THY1+, FACS sorted THY1+, and FACS-sorted GFP+ (FOXC2+) uSPGs simultaneously. To be consistent with the single-cell RNA-seq using the MACS-sorted THY1+ uSPGs, we only presented the results from MACS-sorted THY1+ and FACS-sorted GFP+ (FOXC2+) uSPGs in the previous manuscript. Following the reviewer's suggestion, we have included the results derived from FACS sorted THY1+ uSPGs as the control. The overall conclusion is still fully supported by the more comprehensive dataset, i.e. FOXC2+ cells generated significant higher numbers of colonies than THY1+ cells after transplantation (Figure 2D, E).

> ***Reviewer #2 (Public Review):***

> *The authors found FOXC2 is mainly expressed in As of mouse undifferentiated spermatogonia (uSPG). About 60% of As uSPG were FOXC2+ MKI67-, indicating that FOXC2 uSPG were quiescent. Similar spermatogonia (ZBTB16+ FOXC2+ MKI67-) were also found in human testis.*

> *The lineage tracing experiment using Foxc2iCreERT2/+;Rosa26LSL-T/G/LSL-T/G mice demonstrated that all germ cells were derived from the FOXC2+ uSPG. Furthermore, specific ablation of the FOXC2+ uSPGs using Foxc2iCreERT2/+;Rosa26LSL-DTA/+ mice resulted in the depletion of all uSPG population. In the regenerative condition created by busulfan injection, all FOXC2+ uSPG survived and began to proliferate at around 30 days after busulfan injection. The survived FOXC2+ uSPGs generated all germ cells eventually. To examine the role of FOXC2 in the adult testis, spermatogenesis of Foxc2f/-;Ddx4Cre/+ mice was analyzed. From a 2-month-old, the degenerative seminiferous tubules were increased and became Sertoli cell-only seminiferous tubules, indicating FOXC2 is required to maintain normal spermatogenesis in adult testes. To get insight into the role of FOXC2 in the uSPG, CUT&Tag sequencing was performed in sorted FOXC2+ uSPG from Foxc2iCreERT2/+;Rosa26LSL-T/G/LSL-T/G mice 3 days after TAM diet feeding. The results showed some unique biological processes, including negative regulation of the mitotic cell cycle, were enriched, suggesting the FOXC2 maintains a quiescent state in spermatogonia.*

> *Lineage tracing experiments using transgenic mice of the TAM-inducing system was well-designed and demonstrated interesting results. Based on all data presented, the authors concluded that the FOXC2+ uSPG are primitive SSCs, an indispensable subpopulation to maintain adult spermatogenesis.*

> *The conclusion of the mouse study is mostly supported by the data presented, but to accept some of the authors' claims needs additional information and explanation. Several terminologies define cell populations used in the paper may mislead readers.*

> 1. *"primitive spermatogonial stem cell (SSC)" is confusing. SSCs are considered the most immature subpopulation of uSPG. Thus, primitive uSPGs are likely SSCs. The naming, primitive SSCs, and transit-amplifying SSCs (Figure 7K) are weird. In general, the transit-amplifying cell is progenitor, not stem cell. In human and even mouse, there are several models for the classification of uSPG and SSCs, such as reserved stem cells and active stem cells. The area is highly controversial. The authors' definition of stem cells and progenitor cells should be clarified rigorously and should compare to existing models.*

Thanks for your good comments. Considering that our results showed that FOXC2+ SSCs are in a quiescent state and that Mechanistically FOXC2 maintained the quiescent state of SSCs by promoting the expression of negative regulators of cell cycle, we have replaced 'primitive SSCs' with 'quiescent SSCs' in the revised manuscript. We agree with the reviewer that 'transient amplifying SSCs' is considered to be 'progenitors', thus we have replaced 'transient amplifying SSCs' with 'progenitors' in the revised manuscript. Further，from our point of view, the FOXC2+Ki67+ SSCs could be regarded as active stem cells, and the FOXC2+Ki67- SSCs

could be regarded as reserved stem cells, although further research evidence is still needed to confirm this.

> 1. *scRNA seq data analysis and an image of FOXC2+ ZBTB16+ MKI67- cells by fluorescent immunohistochemistry are not sufficient to conclude that they are human primitive SSCs as described in the Abstract. The identity of human SSCs is controversial. Although Adark spermatogonia are a candidate population of human SSCs, the molecular profile of the Adark spermatogonia seems to be heterogeneous. None of the molecular profiles was defined by a specific cell cycle phase. Thus, more rigorous analysis is required to demonstrate the identity of FOXC2+ ZBTB16+ MKI67- cells and Adark spermatogonia.*

We agree with the reviewer that the identity of human SSCs remain elusive even though Adark population demonstrates certain characteristics of SSCs. To acknowledge this notion, we have revised our conclusion as such that only suggests FOXC2+ZBTB16+MKI67- represents a quiescent state of human SSCs.

> 1. *FACS-sorted GFP+ cells and MACS-THY1 cells were used for functional transplantation assay to evaluate SSC activity. In general, the purity of MACS is significantly lower than that of FACS. Therefore, FACS-sorted THY1 cells must be used for the comparative analysis. As uSPGs in adult testes express THY1, the percentage of GFP+ cells in THY1+ cells determined by flow cytometry is important information to support the transplantation data.*

Thanks for your good comments. According to your suggestions, we have addressed your concerns as follows:

1> The transplantation experiment was conducted using MACS-sorted THY1+, FACS sorted THY1+, and FACS-sorted GFP+ (FOXC2+) uSPGs simultaneously. To be consistent with the single-cell RNA-seq using the MACS-sorted THY1+ uSPGs, we only presented the results from MACS-sorted THY1+ and FACS-sorted GFP+ (FOXC2+) uSPGs in the previous manuscript. Following the reviewer's suggestion, we have included the results derived from FACS sorted THY1+ uSPGs as the control. The overall conclusion is still fully supported by the more comprehensive dataset, i.e. FOXC2+ cells generated significant higher numbers of colonies than THY1+ cells after transplantation (Figure 2D, E).

2> We performed FACS analysis to determine the proportion of GFP+ cells in FACS-sorted THY1+ cells from Rosa26LSL-T/G/LSL-T/G or Foxc2iCreERT2/+;Rosa26LSL-T/G/LSL-T/G mice at day 3 post TAM induction, and the result showed that GFP+ cells account for approximately 20.9±0.21% of THY1+ cells, See Author response image 1.

Author response image 1.

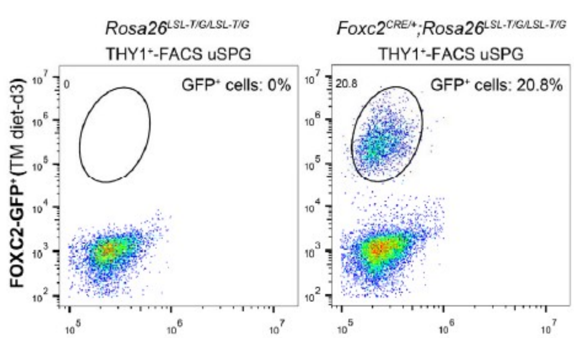

> 1. *The lineage tracing experiments of FOXC2+-SSCs in Foxc2iCreERT2/+;Rosa26LSL-T/G/LSL-T/G showed ~95% of spermatogenic cells and 100% progeny were derived from the FOXC2+ (GFP+) spermatogonia (Figure 2I, J) at month 4 post-TAM induction, although FOXC2+ uSPG were quiescent and a very small subpopulation (~ 60% of As, ~0.03% in all cells). This means that 40% of As spermatogonia and most of Apr/Aal spermatogonia, which were FOXC2 negative, did not contribute to spermatogenesis at all eventually. This is a striking result. There is a possibility that FOXC2CRE expresses more widely in the uSPG population although immunohistochemistry could not detect them.*

Thanks for your good comments. From our lineage tracing results, over 95% of the spermatogenic cells are derived from the FOXC2+ SSCs in the testes of 4-month-old mice, which means that FOXC2+ SSCs maintain a long-term stable spermatogenesis. In addition, previous studies have shown that only a portion of As spermatogonia belong to SSCs with complete self-renewal ability (PMID: 28087628, PMID: 25133429), which is consistent with our findings. Therefore, we speculate that 40% of As spermatogonia and most of Apr/Aal spermatogonia, which were FOXC2 negative, did contribute to spermatogenesis but cannot maintain a long-term spermatogenesis due to limited self-renewal ability.

> 1. *The CUT&Tag_FOXC2 analysis on the FACS-sorted FOXC2+ showed functional enrichment in biological processes such as DNA repair and mitotic cell cycle regulation (Figure 7D). The cells sorted were induced Cre recombinase expression by TAM diet and cut the tdTomato cassette out. DNA repair process and negative regulation of the mitotic cell cycle could be induced by the Cre/lox recombination process. The cells analyzed were not FOXC2+ uSPG in a normal physiological state.*

We do appreciate the reviewer’s concern on the possibility of the functions enriched in the analysis as referred might be derived from Cre/lox recombination. However, we think it is unlikely that the Cre/lox recombination process, supposed to be rather local and specific, can trigger such a systemic and robust response by the DNA damage and cell cycle regulatory pathways. The reasons are as follows: First, as far as we are aware, there has been sufficient data to support this suggested scenario. Second, we did not observe any alteration in either the SSC behaviors or spermatogenesis in general upon the TAM-induced genomic changes, suggesting the impact from the Cre/lox recombination on DNA damage or cell cycle was not significant. Third, no factors associated with the DNA repair process were revealed in the differential analysis of single-cell transcriptomes of FOXC2-WT and FOXC2-KO.

> 1. *Wei et al (Stem Cells Dev 27, 624-636) have published that FOXC2 is expressed predominately in As and Apr spermatogonia and requires self-renewal of mouse SSCs; however, the authors did not mention this study in Introduction, but referred shortly this at the end of Discussion. Their finding should be referred to and evaluated in advance in the Introduction.*

Thanks for your good comments. According to your suggestion, we have revised the introduction to refer this latest parallel work on FOXC2. We are happy to see that our discoveries are converged to the important role of FOXC2 in regulating SSCs in adult mammals.

> ### *Reviewer #3 (Public Review):*

> *By popular single-cell RNA-seq, the authors identified FOXC2 as an undifferentiated spermatogonia-specific expressed gene. The FOXC2+-SSCs can sufficiently initiate and sustain spermatogenesis, the ablation of this subgroup results in the depletion of the uSPG pool. The authors provide further evidence to show that this gene is essential for SSCs maintenance by*

negatively regulating the cell cycle in adult mice, thus well-established FOXC2 as a key regulator of SSCs quiescent state.

The experiments are well-designed and conducted, the overall conclusions are convincing. This work will be of interest to stem cell and reproductive biologists.

Thanks for the positive feedback.

Reviewer #1 (Recommendations for the Authors):

The authors should address the following concerns:

1. *The most primitive uSPGs should be the true SSCs. The term "primitive SSCs" is very confusing.*

1. *In addition to FACS-sorted GFP+ cells, FACS-sorted THY1+ cells should also be used for transplantation.*

Thanks for your good comments. According to your suggestions, we have addressed your two concerns as follows:

1. Overall our work suggest that FOXC2+ SSCs are a subpopulation of SSCs in a quiescent state, thus we have replaced the term 'primitive' with 'quiescent' in the revised manuscript.

2. The transplantation experiment was conducted using MACS-sorted THY1+, FACS sorted THY1+, and FACS-sorted GFP+ (FOXC2+) uSPGs simultaneously. To be consistent with the single-cell RNA-seq using the MACS-sorted THY1+ uSPGs, we only presented the results from MACS-sorted THY1+ and FACS-sorted GFP+ (FOXC2+) uSPGs in the previous manuscript. Following the reviewer's suggestion, we have included the results derived from FACS sorted THY1+ uSPGs as the control. The overall conclusion is still fully supported by the more comprehensive dataset, i.e. FOXC2+ cells generated significant higher numbers of colonies than THY1+ cells after transplantation (Figure 2D, E).

Reviewer #3 (Recommendations for the Authors):

The experiments are well-designed and conducted, the overall conclusions are convincing. The only concerns are the writing, especially the introduction which was not well-rationalized. Sounds the three subtypes and three models for SSCs' self-renew are irrelevant to the major points of this manuscript. I don't think you need to talk too much about the markers of SSCs. Instead, I suggest you provide more background about the quiescent or activation states of the SSCs. In addition to that, as a nuclear-localized protein, it cannot be used to flow cytometric sorting, I don't think it should be emphasized as a marker. You identified a key transcription factor for maintaining the quiescent state of the primitive SSCs, that's quite important!

Appreciate the positive feedback and constructive suggestions on the writing. We have substantially revised our manuscript to include the relevant advances and understanding from the field as well as highlight the importance of FOXC2 in regulating the quiescent state of SSCs.